Council of the European Union

Brussels, 21 December 2020
(OR. en)

14309/20
ADD 1

ENV 835
DELACT 185

COVER NOTE

From:	Secretary-General of the European Commission, signed by Ms Martine DEPREZ, Director
date of receipt:	21 December 2020
To:	Mr Jeppe TRANHOLM-MIKKELSEN, Secretary-General of the Council of the European Union
No. Cion doc.:	C(2020) 9101 final - Annex
Subject:	ANNEX to the Commission Delegated Directive amending, for the purposes of adapting to scientific and technical progress, Annex II to Directive 2002/49/EC of the European Parliament and of the Council as regards common noise assessment methods (Text with EEA relevance)

Delegations will find attached document C(2020) 9101 final - Annex.

Encl.: C(2020) 9101 final - Annex

EUROPEAN
COMMISSION

Brussels, 21.12.2020
C(2020) 9101 final

ANNEX

ANNEX

to the

Commission Delegated Directive

amending, for the purposes of adapting to scientific and technical progress, Annex II to Directive 2002/49/EC of the European Parliament and of the Council as regards common noise assessment methods

(Text with EEA relevance)

EN **EN**

ANNEX

Annex II is amended as follows:

(1)   In Section 2.1.1, the second paragraph, is replaced by the following:

'Calculations are performed in octave bands for road traffic, railway traffic and industrial noise, except for the railway noise source sound power, which uses third octave bands. For road traffic, railway traffic and industrial noise, based on these octave band results, the A-weighted long-term average sound level for the day, evening and night period, as defined in Annex I and referred to in Article 5 of Directive 2002/49/EC, is computed by the method described in sections 2.1.2, 2.2, 2.3, 2.4 and 2.5. For roads and railway traffic in agglomerations, the A-weighted long-term average sound level is determined by the contribution from road and railway segments therein, including major roads and major railways.'

(2)   Section 2.2.1 is amended as follows:

(a)   in the paragraph under the heading "Number and Position of Equivalent Sound Sources", the first sub-paragraph is replaced by the following:

'In this model, each vehicle (category 1, 2, 3, 4 and 5) is represented by one single point source radiating uniformly. The first reflection on the road surface is treated implicitly. As depicted in Figure [2.2.a], this point source is placed 0,05 m above the road surface.'

(b)   in the paragraph under the heading "Sound Power Emission", the last sub-paragraph under the heading "Traffic Flow" is replaced by the following:

'The speed v_m is a representative speed per vehicle category: in most cases the lower of the maximum legal speed for the section of road and the maximum legal speed for the vehicle category.'

(c)   in the paragraph under the heading "Sound Power Emission", the first sub-paragraph under the heading "Individual vehicle" is replaced by the following:

'In the traffic flow, all vehicles of category m are assumed to drive at the same speed, i.e. v_m.'

(3)   Table 2.3.b is amended as follows:

(a)   in the third row, fourth column (called "3"), the text is replaced by the following:

'Represents an indication of the "dynamic" stiffness'

(b)   in the sixth row, fourth column (called "3"), the text is replaced by the following:

'**H**

Hard (800-1000MN/m)'

(4)   Section 2.3.2 is amended as follows:

(a)   in the paragraph under the heading "Traffic Flow", the fourth sub-paragraph, the second indent under formula (2.3.2), is replaced by the following:

'– v is their speed [km/h] in the j-th track section for vehicle type t and average train speed s'

(b)   the paragraph under the headings "Squeal" is replaced by the following:

'Curve squeal is a special source that is only relevant for curves and is therefore localised. Curve squeal is generally dependent on curvature, friction conditions, train speed, track-wheel geometry and dynamics. As it can be significant, an appropriate description is required. At locations where curve squeal occurs, generally in curves and turnouts of railway switches, suitable excess noise power spectra need to be added to the source power. The excess noise may be specific to each type of rolling stock, as certain wheel and bogie types may be significantly less prone to squeal than others. If measurements of the excess noise are available that take sufficiently the stochastic nature of squeal into account, these may be used.

If no appropriate measurements are available, a simple approach can be taken. In this approach, squeal noise shall be considered by adding the following excess values to the rolling noise sound power spectra for all frequencies.

Train	5 dB for curves with 300 m < R ≤ 500m and l_{track} ≥ 50m
	8 dB for curves with R ≤ 300m and l_{track} ≥ 50m
	8 dB for switch turnouts with R ≤ 300m
	0 dB otherwise
Tram	5 dB for curves and switch turnouts with R ≤ 200 m
	0 dB otherwise

where l_{track} is the length of track along the curve and R is the curve radius.

The applicability of these sound power spectra or excess values shall normally be verified on-site, especially for trams and for locations where curves or turnouts are treated with measures against squeal.'

(c)   the paragraph under the headings "Source directivity", directly after equation (2.3.15) the following is added:

'Bridge noise is modelled at source A (h = 1), for which omni-directionality is assumed.'

(d)   the paragraph under the headings "Source Directivity", the second sub-paragraph until and including formula 2.3.16 is replaced by the following:

'*The vertical directivity ΔL $W_{,dir,ver,i}$* in dB is given in the vertical plane for source A (h = 1), as a function of the centre band frequency $f_{c,i}$ of each *i*-th frequency band, and:

for 0 < ψ < π/2 is $$\Delta L_{W,dir,ver,i} = \left(\frac{40}{3} * \left[\frac{2}{3} * \sin(2*\psi) - \sin(\psi)\right] * \lg\left[\frac{f_{c,i}+600}{200}\right]\right)$$ for - π/2< ψ <=0 is $$\Delta L_{W,dir,ver,i} = 0$$	(2.3.16)

'

(5)   In section 2.3.3, the paragraph under the headings "Correction for structural radiation (bridges and viaducts)" is replaced by the following:

'Correction for structural radiation (bridges and viaducts)

In the case where the track section is on a bridge, it is necessary to consider the additional noise generated by the vibration of the bridge as a result of the excitation caused by the presence of the train. The bridge noise is modelled as an additional source of which the sound power per vehicle is given by

$$L_{W,0,bridge,i} = L_{R,TOT,i} + L_{H,bridge,i} + 10 \times \lg(N_a) \, \text{dB}$$	(2.3.18)

where $L_{H,\text{bridge},i}$ is the bridge transfer function. The bridge noise $L_{W,0,\text{bridge},i}$ represents only the sound radiated by the bridge construction. The rolling noise from a vehicle on the bridge is calculated using (2.3.8) through (2.3.10), by choosing the track transfer function that corresponds to the track system that is present on the bridge. Barriers on the edges of the bridge are generally not taken into account.'

(6)   Section 2.4.1 is amended as follows:

(a)   in the paragraph under the headings "Sound Power Emission - general", the second sub-paragraph, the whole fourth element of the list including formula (2.4.1) is replaced by the following:

'-source lines representing moving vehicles are calculated according to formula 2.2.1'

(b)   the number of the formula (2.4.2) is replaced by the following:

'(2.4.1)'

(7)   In section 2.5.1, the seventh paragraph is replaced by the following:

'Objects sloping more than 15° in relation to the vertical are not considered as reflectors but taken into account in all other aspects of propagation, such as ground effects and diffraction.'

(8)   Section 2.5.5 is amended as follows:

(a)   in the paragraph under the headings "Sound level in favourable conditions (LF) for a path (S,R)", the formula 2.5.6 is replaced by the following:

'

$$A_F = A_{div} + A_{atm} + A_{boundary,F}$$	(2.5.6)

'

(b)   in the paragraph under the headings "Long-term sound level at point R in decibels A (dBA)", the end of the first sub-paragraph below the formula 2.5.11, is replaced by the following:

'where i is the index of the frequency band. AWC is the A-weighting correction as follows:

Frequency [Hz]	63	125	250	500	1000	2000	4000	8000
$AWC_{f,I}$ [dB]	-26.2	-16.1	-8.6	-3.2	0	1.2	1.0	-1.1

'

(9)   Section 2.5.6 is amended as follows:

(a)   directly below Figure 2.5.b, the following sentence is added:

'The distances d_n are determined by a 2D projection on the horizontal plane.'

(b)   the sub-paragraph under the headings "Calculation in Favourable Conditions" is amended as follows:

(1)   the first sentence of point (a) is replaced by the following:

'In equation 2.5.15 ($A_{ground,H}$) the heights z_s and z_r are replaced by $z_s + \delta z_s + \delta z_T$ and $z_r + \delta z_r + \delta z_T$ respectively where'

(2)   the first sentence of point (b) is replaced by the following:

'The lower bound of $A_{ground,F}$ (calculated with unmodified heights) depends on the geometry of the path:'

(c)   in the paragraph under the heading "Diffraction", the second sub-paragraph is replaced by the following:

'In practice, the following specifications are considered in the unique vertical plane containing both source and receiver (a flattened Chinese Screen in case of a path including reflections). The direct ray from source to receiver is a straight line under homogeneous propagation conditions and a curved line (arc with radius depending on the length of the straight ray) under favorable propagation conditions.

If the direct ray is not blocked, the edge D is sought which produces the largest path length difference δ (the smallest absolute value because these path length differences are negative). Diffraction is taken into account if

- this path length difference is larger than $-\lambda/20$ and

- if the "Rayleigh-criterion" is fulfilled.

This is the case, if δ is larger than $\lambda/4 - \delta^*$, where δ^* is the path length difference calculated with this same edge D but related to the mirror source S* calculated with the mean ground plane at the source side and the mirror receiver R* calculated with the mean ground plane at

the receiver side. To calculate δ* only the points S*, D and R* are taken into account – other edges blocking the path S*->D->R* are neglected. For the above considerations, the wavelength λ is calculated using the nominal centre frequency and a speed of sound of 340 m/s.

If these two conditions are fulfilled, the edge D separates the source side from the receiver side, two separate mean ground planes are calculated, and A_{dif} is calculated as described in the remainder of this part. Otherwise, no attenuation by diffraction is considered for this path, a common mean ground plane for the path S -> R is calculated, and A_{ground} is calculated with no diffraction ($A_{dif} = 0$ dB). This rule applies in both homogeneous and favourable conditions.'

(d)   in the paragraph under the heading "Pure Diffraction", the second sub-paragraph is replaced by the following:

'For a multiple diffraction, if e is the total path length distance between first and last diffraction point (use curved rays in case of favourable conditions) and if e exceeds 0.3 m (otherwise C'' = 1), this coefficient is defined by:

$$C'' = \frac{1 + \left(5\lambda/e\right)^2}{1/3 + \left(5\lambda/e\right)^2}$$	(2.5.23)

,

(e)   the   Figure   2.5.d   is   replaced   by   the   following:
'

$$\delta = SO + OR - d \qquad\qquad \delta = -(SO + OR - d)$$

$$\delta = SO_1 + e + O_2R - d \qquad\qquad \delta = SO_1 + e + O_2R - d$$

$$\delta = SO_1 + O_1O_2 + O_2O_3 + O_3R - SR$$

'
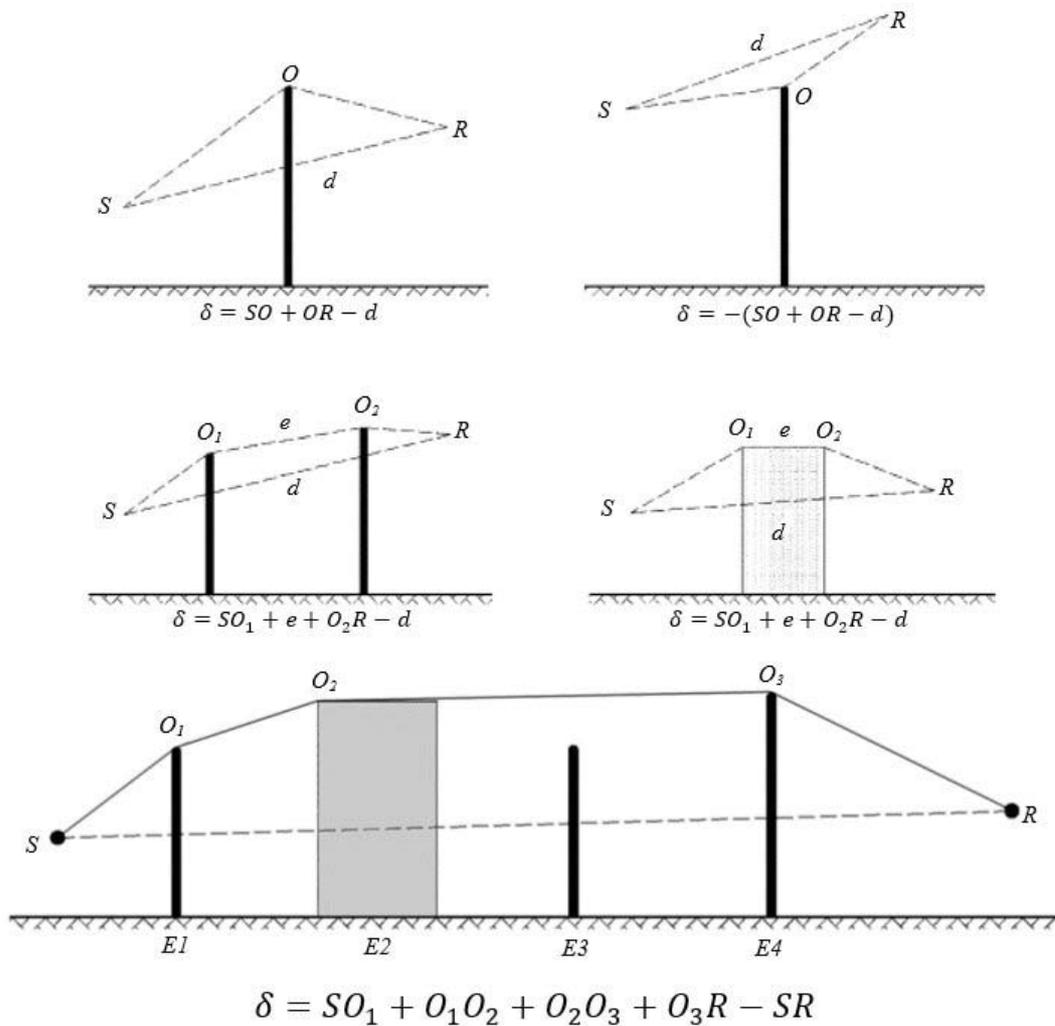
(f)   in the paragraph under the headings "Favourable Conditions", the first sub-paragraph under Figure 2.5.e is replaced by the following:

'In favourable conditions the three curved sound rays *SO*, *OR*, and *SR* have an identical radius of curvature Γ defined by:

$\Gamma = \max(1000, 8d)$	(2.5.24)

Where *d* is defined by the 3D distance between source and receiver of the unfolded path.'

(g)   in the paragraph under the headings "Favourable Conditions", the sub-paragraphs between formula (2.5.28) and formula (2.5.29) (the two formulas included), are replaced by the following:

'

$\delta_F = \hat{S}O + \sum_{i=1}^{n-1} O_i\hat{O}_{i+1} + \hat{O}_nR - \hat{S}R$	(2.5.28)

Under favourable conditions, the propagation path in the vertical propagation plane always consists of segments of a circle whose radius is given by the 3D-distance between source and receiver, that is to say, all segments of a propagation path have the same radius of curvature. If the direct arc connecting source and receiver is blocked, the propagation path is defined as the sho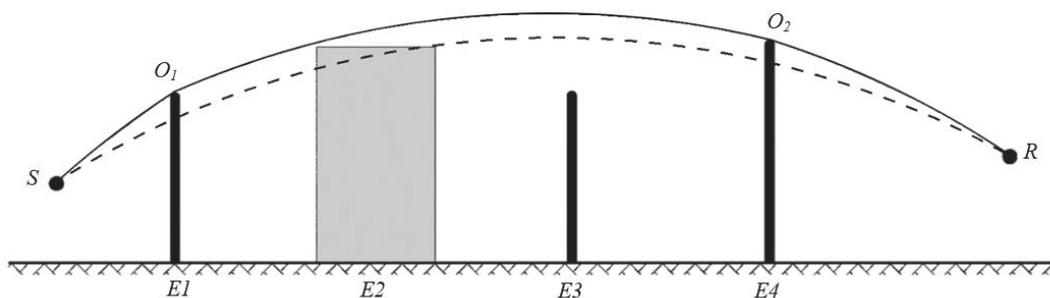rtest convex combination of arcs enveloping all obstacles. Convex in this context means that at each diffraction point, the outgoing ray segment is deflected downward with respect to the incoming ray segment.

Figure 2.5.f

Example of calculation of the path difference in favourable conditions, in the case of multiple diffractions

In the scenario presented in figure 2.5.Figure 2.5.f, the path difference is:

$$\delta_F = \hat{S}O_1 + O_1\hat{O}_2 + \hat{O}_2R - \hat{S}R$$	(2.5.29)

,

(h)   the paragraphs respectively under the headings s "Calculation of the term $\Delta_{ground(S,O)}$" and "Calculation of the term $\Delta_{ground(O,R)}$" are replaced by the following:

'Calculation of the term $\Delta_{ground(S,O)}$

$$\Delta_{ground(S,O)} = -20 \times lg\left(1 + \left(10^{-A_{ground(S,O)}/20} - 1\right) \cdot 10^{-\left(\Delta_{dif(S',R)} - \Delta_{dif(S,R)}\right)/20}\right)$$	(2.5.31)

where

- $A_{ground(S,O)}$ is the attenuation due to the ground effect between the source S and the diffraction point O. This term is calculated as indicated in the previous subsection on calculations in homogeneous conditions and in the previous subsection on calculation in favourable conditions, with the following hypotheses:

- $z_r = z_{o,s}$;

- G_{path} is calculated between S and O;

- In homogeneous conditions: $\bar{G}_w = G'_{path}$ in Equation (2.5.17), $\bar{G}_m = G'_{path}$ in Equation (2.5.18);

- In favourable conditions: $\bar{G}_w = G_{path}$ in Equation (2.5.17), $\bar{G}_m = G'_{path}$ in Equation (2.5.20);

- $\Delta_{dif(S',R)}$ is the attenuation due to the diffraction between the image source *S'* and *R*, calculated as in the previous subsection on *Pure diffraction*;

- $\Delta_{dif(S,R)}$ is the attenuation due to the diffraction between *S* and *R*, calculated as in the previous subsection on *Pure diffraction*.

In the special case where the source lies below the mean ground plane: $\Delta_{dif(S,R)} = \Delta_{dif(S',R)}$ and $\Delta_{ground(S,O)} = A_{ground(S,O)}$

Calculation of the term Δground(O,R)

$$\Delta_{ground(O,R)} = -20 \times lg\left(1 + \left(10^{-A_{ground(O,R)}/20} - 1\right) \cdot 10^{-(\Delta_{dif(S,R')} - \Delta_{dif(S,R)})/20}\right) \qquad (2.5.32)$$

where

- $A_{ground\,(O,R)}$ is the attenuation due to the ground effect between the diffraction point *O* and the receiver *R*. This term is calculated as indicated in the previous subsection on calculation in homogeneous conditions and in the previous subsection on calculation in favourable conditions, with the following hypotheses:

- $z_s = z_{o,r}$

- G_{path} is calculated between *O* and *R*.

The G'_{path} correction does not need to be taken into account here, as the considered source is the diffraction point. Therefore, G_{path} shall indeed be used in the calculation of ground effects, including for the lower bound term of the equation which becomes -3(1-G_{path}).

- In homogeneous conditions, $\bar{G}_w = G_{path}$ in Equation (2.5.17) and $\bar{G}_m = G_{path}$ in Equation (2.5.18);

- In favourable conditions, $\bar{G}_w = G_{path}$ in Equation (2.5.17) and $\bar{G}_m = G_{path}$ in Equation (2.5.20);

- $\Delta_{dif(S,R')}$ is the attenuation due to the diffraction between *S* and the image receiver *R'*, calculated as in the previous section on pure diffraction;

- $\Delta_{dif(S,R)}$ is the attenuation due to the diffraction between *S* and *R*, calculated as in the previous subsection on pure diffraction.

In the special case where the receiver lies below the mean ground plane: $\Delta_{dif(S,R')} = \Delta_{dif(S,R)}$ and $\Delta_{ground(O,R)} = A_{ground(O,R)}$,

(i)   in section 2.5.6, the paragraph under the headings "Vertical Edge Scenarios" is replaced by the following:

'Vertical Edge Scenarios

Equation (2.5.21) may be used to calculate the diffractions on vertical edges (lateral diffractions) in case of industrial noise. If this is the case, $A_{dif} = \Delta_{dif}(S,R)$ is taken and the term A_{ground} is kept. In addition, A_{atm} and A_{ground} shall be calculated from the total length of the propagation path. A_{div} is still calculated from the direct distance d. Equations (2.5.8) and (2.5.6) respectively become:

Δ_{dif} is indeed used in homogeneous conditions in equation   (2.5.34).

$A_H = A_{div} + A_{atm}^{path} + A_{ground,H}^{path} + \Delta_{dif,H(S,R)}$	(2.5.33)

$A_F = A_{div} + A_{atm}^{path} + A_{ground,F}^{path} + \Delta_{dif,H(S,R)}$	(2.5.34)

Lateral diffraction is considered only in cases, where the following conditions are met:

The source is a real point source – not produced by segmentation of an extended source like a line- or area source.

The source is not a mirror source constructed to calculate a reflection.

The direct ray between source and receiver is entirely above the terrain profile.

In the vertical plane containing S and R the path length difference δ is larger than 0, that is to say, the direct ray is blocked. Therefore, in some situations, lateral diffraction may be considered under homogeneous propagation conditions but not under favourable propagation conditions.

If all these conditions are met, up to two laterally diffracted propagation paths are taken into account in addition to the diffracted propagation path in the vertical plane containing source and receiver. The lateral plane is defined as the plane that is perpendicular to the vertical plane and also contains source and receiver. The intersection areas with this lateral plane are constructed from all obstacles that are penetrated by the direct ray from source to receiver. In the lateral plane, the shortest convex connection between source and receiver, consisting of straight segments and encompassing these intersection areas, defines the vertical edges that are taken into account when the laterally diffracted propagation path is constructed.

To calculate ground attenuation for a laterally diffracted propagation path, the mean ground plane between the source and the receiver is calculated taking into account the ground profile vertically below the propagation path. If, in the projection onto a horizontal plane, a lateral propagation path cuts the projection of a building, this is taken into account in the calculation of G_{path} (usually with $G = 0$) and in the calculation of the mean ground plane with the vertical height of the building.'

(j)   in the paragraph under the headings "Reflections on vertical obstacles – Attenuation through absorption", the second and third sub-paragraphs are replaced by the following:

'Surfaces of objects are only considered as reflectors if their slopes are less than 15° with respect to the vertical. Reflections are considered only for paths in the vertical propagation

plane, that is to say, not for laterally diffracted paths. For the incident and reflected paths, and assuming the reflecting surface is to be vertical, the point of reflection (which lays on the reflecting object) is constructed using straight lines under homogeneous and curved lines under favourable propagation conditions. The height of the reflector, when measured through the point of reflection and viewed from the direction of the incident ray, shall be at least 0.5 m. After projection onto a horizontal plane, the width of the reflector when measured through the point of reflection and viewed from the direction of the incident ray, shall be at least 0.5 m.'

(k)   in the paragraph under the headings "Attenuation through retro diffraction", the following is added to the end of the existing text:

'When there is a reflecting noise barrier or obstacle close to the railway track, the sound rays from the source are successively reflected off this obstacle and off the lateral face of the railway vehicle. In these conditions, the sound rays pass between the obstacle and railway vehicle body before diffraction from the top edge of the obstacle.

To take multiple reflections between railway vehicle and a nearby obstacle into account, the sound power of a single equivalent source is calculated. In this calculation, ground effects are ignored.

To derive the sound power of the equivalent source the following definitions apply:

- The origin of the coordinate system is the nearside railhead

- A real source, is located at S (d_s=0, h_s), where h_s is the height of the source relative to the railhead

- The plan h=0 defines the cars' body

- A vertical obstacle with top at B (d_B, h_b)

- A receiver located at a distance $d_R > 0$ behind the obstacle where R has coordinates (d_B+d_R, h_R)

The inner side of the obstacle has absorption coefficients $\alpha(f)$ per octave band. The railway vehicle body has an equivalent reflection coefficient C_{ref}. Normally C_{ref} is equal to 1. Only, in the case of open flat-bed freight wagons a value of 0 can be used. If $d_B>5h_B$ or $\alpha(f)>0.8$ no train barrier interaction is taken into account.

In this configuration, multiple reflections between the railway vehicle body and the obstacle can be calculated using image sources positioned at S_n ($d_n = -2n \cdot d_B, h_n = h_s$), n=0,1,2,..N; as shown in the figure 2.5.k.

Figure 2.5.k
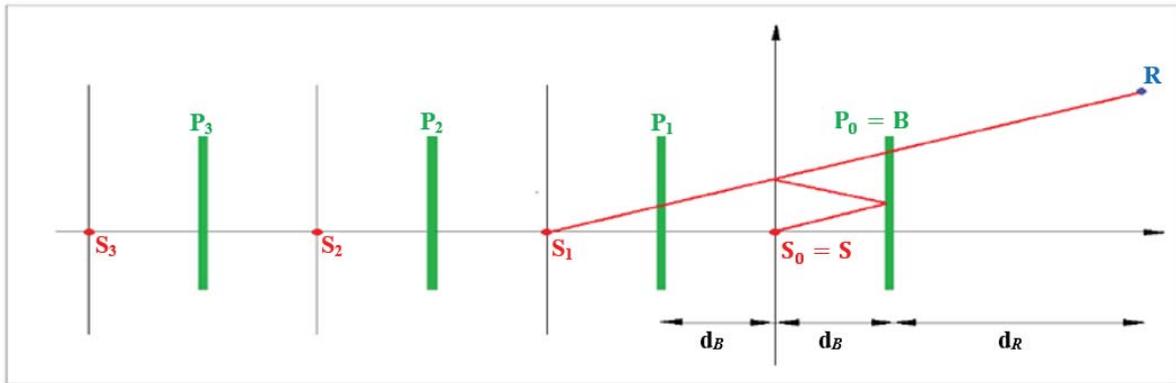
The sound power of the equivalent source is expressed by:

$$L_{W,eq} = 10 \times \lg \left(\sum_{n=0}^{N} 10^{L_{W,n}/10} \right)$$

(2.5.39)

Where the sound power of the partial sources is given by:

$$L_{W,n} = L_W + \Delta L_n$$

$$\Delta L_n = \Delta L_{geo,n} + \Delta L_{dif,n} + \Delta L_{abs,n} + \Delta L_{ref,n} + \Delta L_{retrodif,n}$$

With:

L_W	the sound power of the real source
$\Delta L_{geo,n}$	a correction term for spherical divergence
$\Delta L_{dif,n}$	a correction term for diffraction by the top of the obstacle
$\Delta L_{abs,n}$	a correction term for the absorption at the inner side of the obstacle
$\Delta L_{ref,n}$	a correction term for reflection from the railway vehicle body
$\Delta L_{retrodif,n}$	a correction term for the finite height of the obstacle as a reflector

The correction for spherical divergence is given by

$$\Delta L_{geo,n} = 20 \times \lg \left(\frac{r_0}{r_n} \right)$$

(2.5.40)

$$r_n = |S_n R| = \sqrt{\left(d_n - (d_B + d_R) \right)^2 + (h_n - h_R)^2}$$

(2.5.41)

The correction for diffraction by the top of the obstacle is given by:

(2.5.42)

$$\Delta L_{dif,n} = D_0 - D_n \qquad (2.5.42)$$

Where D_n is the attenuation due to diffraction, calculated by means of formula 2.5.21 where $C'' = 1$, for the path linking source S_n to receiver R, taking into account diffraction at the top of the obstacle B:

$$\delta_n = \pm(|S_n B| + |BR| - |S_n R|) \qquad (2.5.43)$$

The correction for absorption on the inner side of the obstacle is given by:

$$\Delta L_{abs,n} = 10 \cdot n \cdot \lg(1 - \alpha) \qquad (2.5.44)$$

The correction for reflection from the railway vehicle body is given by:

$$\Delta L_{ref,n} = 10 \cdot n \cdot \lg(C_{ref}) \qquad (2.5.45)$$

The correction for the finite height of the reflecting obstacle is taken into account by means of retro-diffraction. The ray path corresponding to an image of order $N > 0$ will be reflected n times by the obstacle. In the cross section, these reflections take place at distances

$d_i = -(2i - q)d_b, i = 1,2,..n$. Where $P_i(d = d_i, h = h_b), i = 1,2,..n$ as the tops of these reflecting surfaces. At each of these points a correction term is calculated as:

$$\Delta L_{retrodif,n} = \begin{cases} -\sum\limits_{i=1}^{n} \Delta_{retrodif,n,i} & if\ n > 0 \\ 0 & if\ n = 0 \end{cases} \qquad (2.5.46)$$

Where $\Delta_{retrodif,n,i}$ is calculated for a source at position S_n an obstacle top at P_i and a receiver at position R'. The position of the equivalent receiver R' is given by $R'=R$ if the receiver is above line of sight from S_n to B; otherwise the equivalent receiver position is taken on the line of sight vertically above the real receiver; namely:

$$d_{R'} = d_R$$	(2.5.47)

$$h_{R'} = max\left(h_R, h_B \frac{d_B + d_R - d_n}{d_B - d_n}\right)$$	(2.5.48)

'

(10)   Section 2.7.5 'Aircraft noise and performance', is replaced by the following:

'*2.7.5 Aircraft noise and performance*

The ANP database provided in Appendix I contains aircraft and engine performance coefficients, departure and approach profiles as well as NPD relationships for a substantial proportion of civil aircraft operating from European Union airports. For aircraft types or variants for which data are not currently listed, they can best be represented by data for other, normally similar, aircrafts that are listed.

This data was derived to calculate noise contours for an average or representative fleet and traffic mix at an airport. It may not be appropriate to predict absolute noise levels of an individual aircraft model and is not suitable to compare the noise performance and characteristics of specific aircraft types, models or a specific fleet of aircraft. Instead, to determine which aircraft types, models or specific fleet of aircrafts are the noisiest contributors, the noise certificates shall be looked at.

The ANP database includes one or several default take-off and landing profiles for each aircraft type listed. The applicability of these profiles to the airport under consideration shall be examined, and either the fixed-point profiles or the procedural steps that best represent the flight   operations   at   this   airport   shall   be   determined.'

(11)   In Section 2.7.11, the title of the second paragraph under the headings 'Track dispersion' is replaced by the following:

'*Lateral track dispersion*'

(12)   In section 2.7.12, after the sixth sub-paragraph and before the seventh and last sub-paragraph, the following sub-paragraph is inserted:

'An aircraft noise source should be entered at a minimum height of 1.0 m (3.3 ft) above the aerodrome level, or above the terrain elevation levels of the runway, as relevant.'

(13)   Section 2.7.13, '*Construction of flight path segments*', is replaced by the following:
'

2.7.13 Construction of flight path segments

Each flight path has to be defined by a set of segment coordinates (nodes) and flight parameters. The starting point is to determine the co-ordinates of the ground track segments. The flight profile is then calculated, remembering that for a given set of procedural steps, the profile depends on the ground track; e.g. at the same thrust and speed the aircraft climb rate is less in turns than in straight flight. Sub-segmentation is then undertaken for the aircraft on the runway (takeoff or landing ground roll), and for the aircraft near to the runway (initial climb or final approach). Airborne segments with significantly different speeds at their start and end points should then be sub-segmented. The two-dimensional co-ordinates of the ground track[1] segments are determined and merged with the two-dimensional flight profile to construct the three-dimensional flight path segments. Finally, any flight path points that are too close together are removed.

Flight profile

The parameters describing each flight profile segment at the start (suffix 1) and end (suffix 2) of the segment are:

s_1, s_2 distance along the ground track,

z_1, z_2 aeroplane height,

V_1, V_2 groundspeed,

P_1, P_2 noise-related power parameter (matching that for which the NPD-curves are defined), and

$\varepsilon_1, \varepsilon_2$ bank angle.

To build a flight profile from a set of procedural steps (*flight path synthesis*), segments are constructed in sequence to achieve required conditions at the end points. The end-point parameters for each segment become the start-point parameters for the next segment. In any segment calculation the parameters are known at the start; required conditions at the end are specified by the procedural step. The steps themselves are defined either by the ANP defaults or by the user (e.g. from aircraft flight manuals). The end conditions are usually height and speed; the profile building task is to determine the track distance covered in reaching those conditions. The undefined parameters are determined via flight performance calculations described in **Appendix B**.

If the ground track is straight, the profile points and associated flight parameters can be determined independently of the ground track (bank angle is always zero). However ground tracks are rarely straight; they usually incorporate turns and, to achieve best results, these have to be accounted for when determining the 2-dimensional flight profile, where necessary splitting profile segments at ground track nodes to inject changes of bank angle. As a rule the length of the next segment is unknown at the outset and it is calculated provisionally

---

[1]   For this purpose the total length of the ground track should always exceed that of the flight profile. This can be achieved, if necessary, by adding straight segments of suitable length to the last segment of the ground track.

assuming no change of bank angle. If the provisional segment is then found to span one or more ground track nodes, the first being at s, namely $s_1 < s < s_2$, the segment is truncated at s, calculating the parameters there by interpolation (see below). These become the end-point parameters of the current segment and the start-point parameters of a new segment - which still has the same target end conditions. If there is no intervening ground track node the provisional segment is confirmed.

If the effects of turns on the flight profile are to be disregarded, the straight flight, single segment solution is adopted although the bank angle information is retained for subsequent use.

Whether or not turn effects are fully modelled, each 3-dimensional flight path is generated by merging its 2-dimensional flight profile with its 2-dimensional ground track. The result is a sequence of co-ordinate sets (x,y,z), each being either a node of the segmented ground track, a node of the flight profile or both, the profile points being accompanied by the corresponding values of height z, ground speed V, bank angle ε and engine power P. For a track point (x,y) which lies between the end points of a flight profile segment, the flight parameters are interpolated as follows:

$$z = z_1 + f \cdot (z_2 - z_1)$$	(2.7.3)
$$V = \sqrt{V_1{}^2 + f \cdot (V_2{}^2 - V_1{}^2)}$$	(2.7.4)
$$\varepsilon = \varepsilon_1 + f \cdot (\varepsilon_2 - \varepsilon_1)$$	(2.7.5)
$$P = \sqrt{P_1{}^2 + f \cdot (P_2{}^2 - P_1{}^2)}$$	(2.7.6)

where

$$f = (s - s_1)/(s_2 - s_1)$$	(2.7.7)

Note that whilst z and ε are assumed to vary linearly with distance, V and P are assumed to vary linearly with time (namely constant acceleration[2]).

When matching flight profile segments to radar data (*flight path analysis*) all end-point distances, heights, speeds and bank angles are determined directly from the data; only the power settings have to be calculated using the performance equations. As the ground track and flight profile coordinates can also be matched appropriately, this is usually quite straightforward.

Takeoff ground roll

When taking off, as an aircraft accelerates between the point of brake release (alternatively termed Start-of-Roll *SOR*) and the point of lift-off, speed changes dramatically over a distance of 1500 to 2500 m, from zero to between around 80 and 100 m/s.

---

[2] Even if engine power settings remain constant along a segment, propulsive force and acceleration can change due to variation of air density with height. However, for the purposes of noise modelling these changes are normally negligible.

The takeoff roll is thus divided into segments with variable lengths over each of which the aircraft speed changes by specific increment ΔV of no more than 10 m/s (about 20kt). Although it actually varies during the takeoff roll, an assumption of constant acceleration is adequate for this purpose. In this case, for the takeoff phase, V_1 is initial speed, V_2 is the takeoff speed, n_{TO} is the number of takeoff segment and s_{TO} is the equivalent takeoff distance. For equivalent takeoff distance s_{TO} (see **Appendix B**) and takeoff speed V_1 and takeoff speed V_{TO} the number n_{TO} of segments for the ground roll is

| $$n_{TO} = int(1 + (V_{TO} - V_1)/10)$$ | (2.7.8) |

and hence the change of velocity along a segment is

| $$\Delta V = V_{TO}/n_{TO}$$ | (2.7.9) |

and the time Δt on each segment is (constant acceleration assumed)

| $$\Delta_t = \frac{2 \cdot s_{TO}}{V_{TO} \cdot n_{TO}}$$ | (2.7.10) |

The length $s_{TO,k}$ of segment k ($1 \leq k \leq n_{TO}$) of the takeoff roll is then:

| $$s_{TO,k} = (k - 0.5) \cdot \Delta V \cdot \Delta t = \frac{(2k - 1) \cdot s_{TO}}{n_{TO}^2}$$ | (2.7.11) |

Example: For a takeoff distance $s_{TO} = 1600$ m, $V_1 = 0$m/s and $V_2 = 75$ m/s, this yields $n_{TO} = 8$ segments with lengths ranging from 25 to 375 meters (see **Figure 2.7.g**):

Figure 2.7.g

Segmentation of a takeoff roll (example for 8 segments)
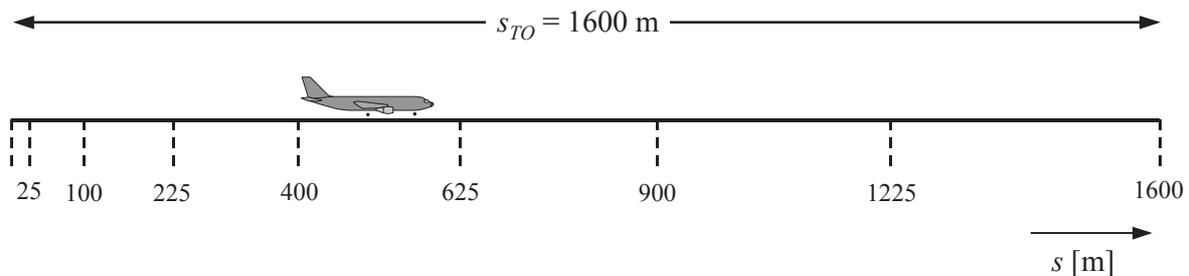
Similarly to the speed changes, the aircraft thrust changes over each segment by a constant increment ΔP, calculated as

| $$\Delta P = (P_{TO} - P_{init})/n_{TO}$$ | (2.7.12) |

where P_{TO} and P_{init} respectively designate the aircraft thrust at the point of lift-off and the aircraft thrust at the start of takeoff roll.

The use of this constant thrust increment (instead of using the quadratic form equation 2.7.6) aims at being consistent with the linear relationship between thrust and speed in the case of jet-engine aircraft.

Important note: The above equations and example implicitly assume that the initial speed of the aircraft at the start of the takeoff phase is zero. This corresponds to the common situation where the aircraft starts to roll and accelerate from the brake release point. However, there are also situations where the aircraft may start to accelerate from its taxiing speed, without stopping at the runway threshold. In that case of non-zero initial speed V_{init}, the following 'generalised' equations should be used in replacement of equations 2.7.8, 2.7.9. 2.7.10 and 2.7.11.

$$\begin{cases} n_{TO} = int(1 + |V_2 - V_1|/10) \\ \Delta V = (V_2 - V_1)/n \\ \Delta t = \dfrac{2 \cdot s}{(V_2 + V_1) \cdot n} \\ s_k = \left(V_1 + \Delta V \cdot (k - 0.5)\right) \cdot \dfrac{2 \cdot s}{(V_2 + V_1) \cdot n} \end{cases} \qquad (2.7.13)$$

In this case, for the takeoff phase, V_1 is initial speed V_{init}, V_2 is the takeoff speed V_{TO}, n is the number of takeoff segment n_{TO}, s is the equivalent takeoff distance s_{TO} and s_k is the length $s_{TO,k}$ of segment k (1 [Symbol] k [Symbol] n).

The landing ground roll

Although the landing ground roll is essentially a reversal of the takeoff ground roll, special account has to be taken of

- *reverse thrust* which is sometimes applied to decelerate the aircraft and

- aeroplanes leaving the runway after deceleration (aircraft that leave the runway no longer contribute to air noise as noise from taxiing is disregarded).

In contrast to the takeoff roll distance, which is derived from aircraft performance parameters, the stop distance s_{stop} (namely the distance from touchdown to the point where the aircraft leaves the runway) is not purely aircraft specific. Although a minimum stop distance can be estimated from aircraft mass and performance (and available reverse thrust), the actual stop distance depends also on the location of the taxiways, on the traffic situation, and on airport-specific regulations on the use of reverse thrust.

The use of reverse thrust is not a standard procedure - it is only applied if the needed deceleration cannot be achieved by the use of the wheel brakes. (Reverse thrust can be exceptionally disturbing as a rapid change of engine power from idle to reverse settings produces a sudden burst of noise.)

However, most runways are used for departures as well as for landings so that reverse thrust has a very small effect on the noise contours since the total sound energy in the vicinity of the

runway is dominated by the noise produced from takeoff operations. Reverse thrust contributions to contours may only be significant when runway use is limited to landing operations.

Physically, reverse thrust noise is a very complex process but because of its relatively minor significance to air noise contours it can be modelled simplistically - the rapid change in engine power being taken into account by suitable segmentation.

It is clear that modelling the landing ground roll is less straightforward than for takeoff roll noise. The following simplified modelling assumptions are recommended for general use, when no detailed information is available (see **Figure 2.7.h.1**).

Figure 2.7.h.1

Modelling of landing ground roll
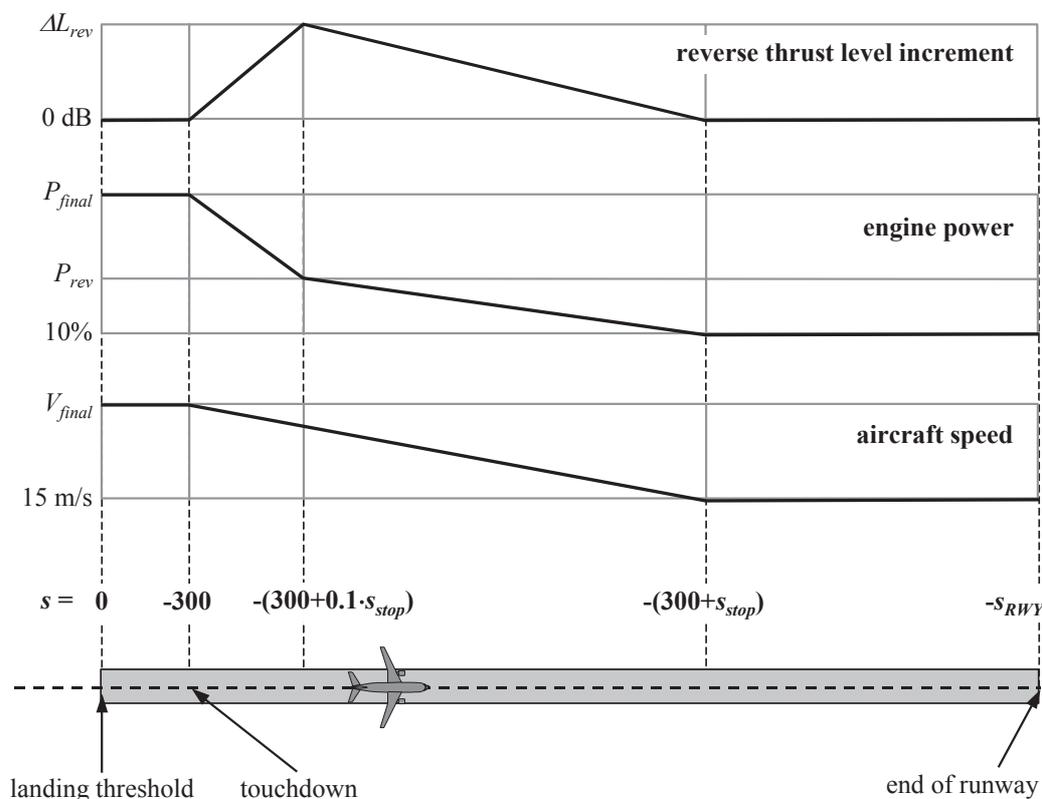
The aircraft crosses the landing threshold (which has the co-ordinate $s = 0$ along the approach ground track) at an altitude of 50 feet, and then continues to descend on its glideslope until it touches down on the runway. For a 3° glideslope, the touch-down point is 291 m beyond the landing threshold (as illustrated in Figure 2.7.h.1). The aircraft is then decelerated over a stop-distance s_{stop} - aircraft specific values of which are given in the ANP database - from final approach speed V_{final} to 15 m/s. Because of the rapid changes in speed during this segment it should be sub-segmented in the same manner as for the takeoff ground roll (or airborne segments with rapid speed changes), using the generalised equations 2.7.13 (as taxi-in speed is not equal to zero). The engine power changes from final approach power at touchdown to a reverse thrust power setting P_{rev} over a distance $0.1 \cdot s_{stop}$, then decreases to 10 % of the maximum available power over the remaining 90 percent of the stop distance. Up to the end of the runway (at $s = -s_{RWY}$) aircraft speed remains constant.

NPD curves for reverse thrust are not at present included in the ANP database, and it is therefore necessary to rely on the conventional curves for modelling this effect. Typically the reverse thrust power P_{rev} is around 20% of the full power setting and this is recommended when no operational information is available. However, at a given power setting, reverse thrust tends to generate significantly more noise than forward thrust and an increment ΔL shall be applied to the NPD-derived event level, increasing from zero to a value ΔL_{rev} (5dB is recommended provisionally[3]) along $0.1 \cdot s_{stop}$ and then falling linearly to zero along the remainder of the stop distance.

Segmentation of the initial climb and final approach segments

The segment-to-receiver geometry changes rapidly along the initial climb and final approach airborne segments, particularly with respect to observer locations to the side of the flight track, where the elevation angle (*beta angle*) also changes rapidly as the aircraft climbs or descends through these initial/final segments. Comparisons with very small segment calculations show that using a single (or a limited number of) climb or approach airborne segment(s) below a certain height (relative to the runway) results in a poor approximation of noise to the side of the flight track for integrated metrics. This is due to the application of a single lateral attenuation adjustment on each segment, corresponding to a single segment-specific value of the elevation angle, whereas the rapid change of this parameter results in significant variations of the lateral attenuation effect along each segment. Calculation accuracy is improved by sub-segmenting the initial climb and last approach airborne segments. The number of sub-segments and the length of each determine the lateral attenuation change 'granularity' which will be accounted for. Noting the expression of total lateral attenuation for aircraft with fuselage-mounted engines, it can be shown that for a limiting change in lateral attenuation of 1.5 dB per sub-segment, the climb and approach airborne segments located below a height of 1289.6 m (4231 ft) above the runway should be sub-segmented based on the following set of height values:

z = {18.9, 41.5, 68.3, 102.1, 147.5, 214.9, 334.9, 609.6, 1289.6} metres, or

z = {62, 136, 224, 335, 484, 705, 1099, 2000, 4231} feet

For each original segment below 1289.6 m (4231 ft), the above heights are implemented by identifying which height in the set above is closest to the original endpoint height (for a climb segment) or start-point height (for an approach segment). The actual sub-segment heights, z_i, would then be calculated using:

$z_i = z_e \left[z'_i / z'_N \right]$ (i = k..N)

where:

z_e	is the original segment endpoint height (climb) or start-point height (approach)
z'_i	is the ith member of the set of height values listed above
z'_N	is the closest height from the set of height values listed above to height z_e

---

[3] This was recommended in the previous edition of ECAC Doc 29 but is still considered provisional pending the acquisition of further corroborative experimental data.

k denotes the index of the first member of the set of height values for which the calculated z_k is strictly greater than the endpoint height of the previous original climb segment or the start-point height of the next original approach segment to be sub-segmented.

In the specific case of an initial climb segment or last approach segment, $k = 1$, but in the more general case of airborne segments not connected to the runway, k will be greater than 1.

Example for an initial climb segment:

If the original segment endpoint height is $z_e = 304.8$ m, then from the set of height values, 214.9 m $< z_e < 334.9$ m and the closest height from the set to z_e is $z'_7 = 334.9$ m. The sub-segment endpoint heights are then computed by:

$z_i = 304.8 [z'_i / 334.9]$ for $i = 1$ to 7

(noting that $k = 1$ in that case, as this is an initial climb segment)

Thus z_1 would be 17.2 m and z_2 would be 37.8 m, etc.

Segmentation of airborne segments

For airborne segments where there is a significant speed change along a segment, this shall be subdivided as for the ground roll, namely

$$n_{seg} = int(1 + |V_2 - V_1|/10)$$	(2.7.14)

where V_1 and V_2 are the segment start and end speeds respectively. The corresponding sub-segment parameters are calculated in a similar manner as for the takeoff ground roll, using equations 2.7.9 to 2.7.11.

Ground track

A ground track, whether a backbone track or a dispersed sub-track, is defined by a series of (x,y) co-ordinates in the ground plane (e.g. from radar information) or by a sequence of vectoring commands describing straight segments and circular arcs (turns of defined radius r and change of heading $\Delta\xi$).

For segmentation modelling, an arc is represented by a sequence of straight segments fitted to sub-arcs. Although they do not appear explicitly in the ground-track segments, the banking of aircraft during turns influences their definition. **Appendix B4** explains how to calculate bank angles during a steady turn but of course these are not actually applied or removed instantaneously. How to handle the transitions between straight and turning flight, or between one turn and an immediately sequential one, is not prescribed. As a rule, the details, which are left to the user (see **section 2.7.11**), are likely to have a negligible effect on the final contours; the requirement is mainly to avoid sharp discontinuities at the ends of the turn and this can be achieved simply, for example, by inserting short transition segments over which the bank angle changes linearly with distance. Only in the special case that a particular turn is likely to have a dominating effect on the final contours would it be necessary to model the dynamics of the transition more realistically, to relate bank angle to particular aircraft types and to adopt

appropriate roll rates. Here it is sufficient to state that the end sub-arcs $\Delta\xi_{trans}$ in any turn are dictated by bank angle change requirements. The remainder of the arc with change of heading $\Delta\xi - 2\cdot\Delta\xi_{trans}$ degrees is divided into n_{sub} sub-arcs according to the equation:

$$n_{sub} = int(\, 1 + (\Delta\xi - 2\cdot\Delta\xi_{trans})/10\,) \qquad (2.7.15)$$

where int(x) is a function that returns the integer part of x. Then the change of heading $\Delta\xi_{sub}$ of each sub-arc is computed as

$$\Delta\xi = (\xi - 2\cdot\Delta\xi_{trans})/n_{sub} \qquad (2.7.16)$$

where n_{sub} needs to be large enough to ensure that $\Delta\xi_{sub} \leq 10$ degrees. The segmentation of an arc (excluding the terminating transition sub-segments) is illustrated in **Figure 2.7.h.2**[4].

Figure 2.7.h.2

Construction of flight path segments dividing turn into segments of length Δs (upper view in horizontal plane, lower view in vertical plane)

---
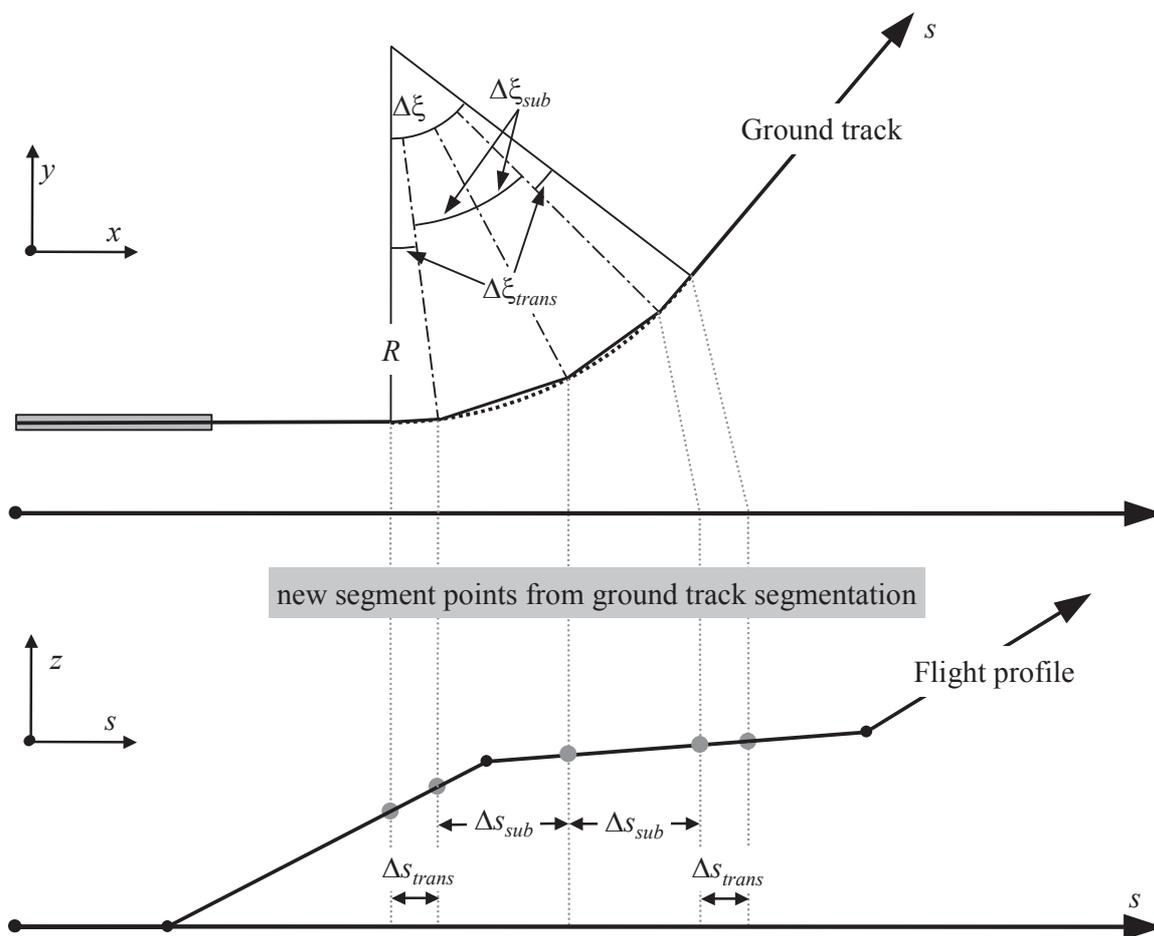
[4]   Defined in this simple way, the total length of the segmented path is slightly less than that of the circular path. However the consequent contour error is negligible if the angular increments are below 30°.

Once the ground track segments have been established in the x-y plane, the flight profile segments (in the s-z plane) are overlaid to produce the three-dimensional (x, y, z) track segments.

The ground track should always extend from the runway to beyond the extent of the calculation grid. This can be achieved, if necessary, by adding a straight segment of suitable length to the last segment of the ground track.

The total length of the flight profile, once merged with the ground track, must also extend from the runway to beyond the extent of the calculation grid. This can be achieved, if necessary, by adding an extra profile point:

- to the end of a departure profile with speed and thrust values equal to those of the last departure profile point, and height extrapolated linearly from the last and penultimate profile points; or

- to the beginning of an arrival profile with speed and thrust value equal to those of the first arrival profile point, and height extrapolated linearly back from the first and second profile points.

Segmentation adjustments of airborne segments

After the 3-D flight path segments have been derived according to the procedure described in **Section 2.7.13**, further segmentation adjustments may be necessary to remove flight path points which are too close together.

When adjacent points are within 10 metres of each other, and when the associated speeds and thrusts are the same, one of the points should be eliminated.'

(14)   Section 2.7.16. '*Determination of event levels from NPD-data*', is replaced by the following:

'*2.7.16 Determination of event levels from NPD-data*

The principal source of aircraft noise data is the international Aircraft Noise and Performance (ANP) database. This tabulates L_{max} and L_E as functions of propagation distance d - for specific aircraft types, variants, flight configurations (approach, departure, flap settings), and power settings P. They relate to steady flight at specific reference speeds V_{ref} along a notionally infinite, straight flight path[5].

How values of the independent variables P and d are specified is described later. In a single look-up, with input values P and d, the output values required are the *baseline levels $L_{max}(P,d)$* and/or $L_{E\infty}(P,d)$ (applicable to an infinite flight path). Unless values happen to be tabulated for P and/or d exactly, it will generally be necessary to estimate the required event noise level(s) by interpolation. A linear interpolation is used between tabulated power-settings, whereas a logarithmic interpolation is used between tabulated distances (see **Figure 2.7.i**).

---

[5] Although the notion of an infinitely long flight path is important to the definition of event sound exposure level L_E, it has less relevance in the case of event maximum level L_{max} which is governed by the noise emitted by the aircraft when at a particular position at or near its closest point of approach to the observer. For modelling purposes the NPD distance parameter is taken to be the minimum distance between the observer and segment.

Figure 2.7.i

Interpolation in noise-power-distance curves
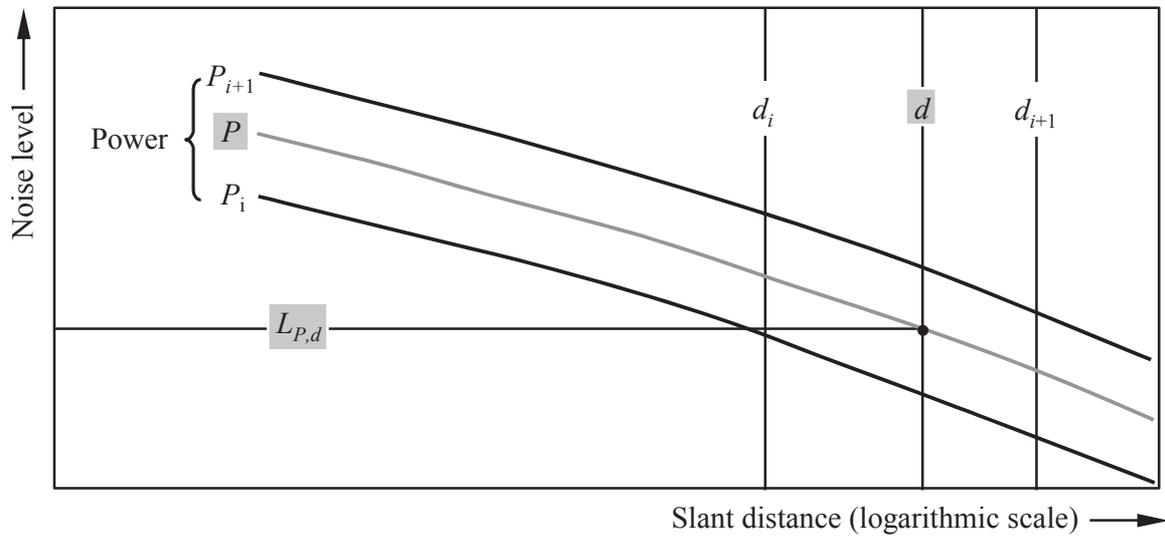
If P_i and P_{i+1} are engine power values for which noise level versus distance data are tabulated, the noise level $L(P)$ at a given distance for intermediate power P, between P_i and P_{i+1}, is given by:

$$L(P) = L(P_i) + \frac{L(P_{i+1}) - L(P_i)}{P_{i+1} - P_i} \cdot (P - P_i) \qquad (2.7.19)$$

If, at any power setting, d_i and d_{i+1} are distances for which noise data are tabulated, the noise level $L(d)$ for an intermediate distance d, between d_i and d_{i+1} is given by

$$L(d) = L(d_i) + \frac{L(d_{i+1}) - L(d_i)}{\log d_{i+1} - \log d_i} \cdot (\log d - \log d_i) \qquad (2.7.20)$$

By using equations (2.7.19) and (2.7.20), a noise level $L(P,d)$ can be obtained for any power setting P and any distance d that is within the envelope of the NPD data base.

For distances d that lie outside the NPD envelope, equation 2.7.20 is used to extrapolate from the last two values, namely inwards from $L(d_1)$ and $L(d_2)$ or outwards from $L(d_{I-1})$ and $L(d_I)$ where I is the total number of NPD points on the curve. Thus

Inwards:

$$L(d) = L(d_2) + \frac{L(d_1) - L(d_2)}{\log d_2 - \log d_1} \cdot (\log d_2 - \log d) \qquad (2.7.21)$$

Outwards:

$$L(d) = L(d_{I-1}) - \frac{L(d_{I-1}) - L(d_I)}{\log d_I - \log d_{I-1}} \cdot (\log d - \log d_{I-1})$$

(2.7.22)

As, at short distances d, noise levels increase very rapidly with decreasing propagation distance, it is recommended that a lower limit of 30 m be imposed on d, namely $d = \max(d, 30\text{ m})$.

Impedance adjustment of standard NPD data

The NPD data provided in the ANP database are normalized to reference atmospheric conditions (temperature of 25°C and pressure of 101.325 kPa). Before applying the interpolation/extrapolation method previously described, an acoustic impedance adjustment shall be applied to these standard NPD data.

Acoustic impedance is related to the propagation of sound waves in an acoustic medium, and is defined as the product of the density of air and the speed of sound. For a given sound intensity (power per unit area) perceived at a specific distance from the source, the associated sound pressure (used to define SEL and L_{Amax} metrics) depends on the acoustic impedance of the air at the measurement location. It is a function of temperature, atmospheric pressure (and indirectly altitude). There is therefore a need to adjust the standard NPD data of the ANP database to account for the actual temperature and pressure conditions at the receiver point, which are generally different from the normalized conditions of the ANP data.

The impedance adjustment to be applied to the standard NPD levels is expressed as follows:

$$\Delta_{Impedance} = 10 \cdot lg \left(\frac{\rho \cdot c}{409.81} \right)$$

(2.7.23)

where:

$\Delta_{Impedance}$	Impedance adjustment for the actual atmospheric conditions at the receiver point (dB)
$\rho \cdot c$	Acoustic impedance (newton · seconds/m³) of the air at the aerodrome elevation (409.81 being the air impedance associated to the reference atmospheric conditions of the NPD data in the ANP database).

Impedance $\rho \cdot c$ is calculated as follows:

$$\rho \cdot c = 416.86 \cdot \left[\frac{\delta}{\theta^{1/2}} \right]$$

(2.7.24)

δ	p/po, the ratio of the ambient air pressure at the observer altitude to the standard air pressure at mean sea level: p_0 = 101.325 kPa (or 1013.25 mb)

θ (T + 273.15)/(T$_0$ + 273.15) the ratio of the air temperature at the observer altitude to the standard air temperature at mean sea level: $T_0 = 15.0\ °C$

The acoustic impedance adjustment is usually less than a few tenths of one dB. In particular, it should be noted that under the standard atmospheric conditions (p_0 = 101.325 kPa and T_0 = 15.0 °C), the impedance adjustment is less than 0.1 dB (0.074 dB). However, when there is a significant variation in temperature and atmospheric pressure relative to the reference atmospheric conditions of the NPD data, the adjustment can be more substantial.'

(15)   In Section 2.7.18. '*Flight path segment parameters*', the paragraph under the headings 'Segment power P' is replaced by the following:

'

Segment power P

The tabulated NPD data describe the noise of an aircraft in steady straight flight on an infinite flight path, that is to say, at constant engine power *P*. The recommended methodology breaks actual flight paths, along which speed and direction vary, into a number of finite segments, each of which is then taken to be part of a uniform, infinite flight path for which the NPD data are valid. But the methodology provides for changes of power along the length of a segment; it is taken to change quadratically with distance from *P₁* at its start to *P₂* at its end. It is therefore necessary to define an equivalent steady segment value *P*. This is taken to be the value at the point on the segment that is closest to the observer. If the observer is alongside the segment (Figure 2.7.k) it is obtained by interpolation as given by equation 2.7.8 between the end values, namely

$$P = \sqrt{P_1{}^2 + \frac{q}{\lambda} \cdot \left(P_2{}^2 - P_1{}^2\right)}$$
(2.7.31)

If the observer is behind or ahead of the segment, it is that at the nearest end point, *P₁* or *P₂*.'

(16)   Section 2.7.19 is amended as follows

(a)   in the paragraph under the headings '*The duration correction DV (Exposure levels LE only)* until and including the formula 2.7.34 is replaced by the following:

'*The duration correction ΔV (Exposure levels LE only)*

This correction[6] accounts for a change in exposure levels if the actual segment groundspeed is different to the aircraft reference speed V_{ref} to which the basic NPD-data relate.

Like engine power, speed varies along the flight path segment (from V$_{T1}$ to V$_{T2}$, which are the speeds output from Appendix B or from a previously pre-calculated flight profile).

---

[6]   This is known as the *duration correction* because it makes allowance for the effects of aircraft *speed* on the duration of the sound event - implementing the simple assumption that, other things being equal, duration, and thus received event sound energy, is inversely proportional to source velocity.

For airborne segments, V_{seg} is the segment speed at the closest point of approach, **S**, interpolated between the segment end-point values assuming it varies quadratically with time; namely if the observer is alongside the segment:

$$V_{seg} = \sqrt{V_1{}^2 + \frac{q}{\lambda} \cdot \left(V_2{}^2 - V_1{}^2\right)} \qquad (2.7.32)$$

'

(b)   the formula numbers "(2.7.35)", "(2.7.36)" and "(2.7.37)", are respectively replaced by the following other numbers:

'(2.7.33)', '(2.7.34)' and '(2.7.35)'.

(c)   the following first two words of the paragraph under the headings "Sound propagation geometry" are replaced by the following:

'Figure 2.7.m'

(d)   the table in the second subparagraph is replaced by the following:

'

$a = 0.00384,$	$b = 0.0621,$	$c = 0.8786$	for wing-mounted engines and	(2.7.36)
$a = 0.1225,$	$b = 0.3290,$	$c = 1$	for fuselage-mounted engines.	(2.7.37)

'

(e)   the text under the Figure 2.7.p is replaced by the following:

'To calculate the lateral attenuation using equation (2.7.40) (where β is measured in a vertical plane), an extended *level* flight path is recommended. An extended level flight path is defined in the vertical plane through **S₁S₂** and with the same perpendicular slant distance d_p from the observer. This is visualised by rotating the triangle **ORS**, and its attached flight path about **OR** (see **Figure 2.7p**) through angle γ thus forming the triangle **ORS´**. The elevation angle of this equivalent level path (now in a vertical plane) is $\beta = \tan^{-1}(h/\ell)$ (ℓ remains unchanged). In this case, for an observer alongside, angle β and the resulting lateral attenuation $\Lambda(\beta,\ \ell)$ are the same for L_E and L_{max} metrics.

Figure 2.7.r illustrates the situation when the observer point **O** lies *behind the finite segment*, not alongside. Here the segment is observed as a more distant part of an infinite path; a perpendicular can only be drawn to point **S$_p$** on its extension. The triangle **OS₁S₂** accords with **Figure 2.7.j** which defines the segment correction Δ_F. But in this case the parameters for lateral directivity and attenuation are less obvious.

Figure 2.7.r

Observer behind segment

γ = climb angle
ε = bank angle
β = elevation angle for L_E = $\tan^{-1}(h/\ell)$
β_1 = elevation angle for L_{max} = $\sin^{-1}(z_1/d_1)$
φ = depression angle = $\beta - \varepsilon$
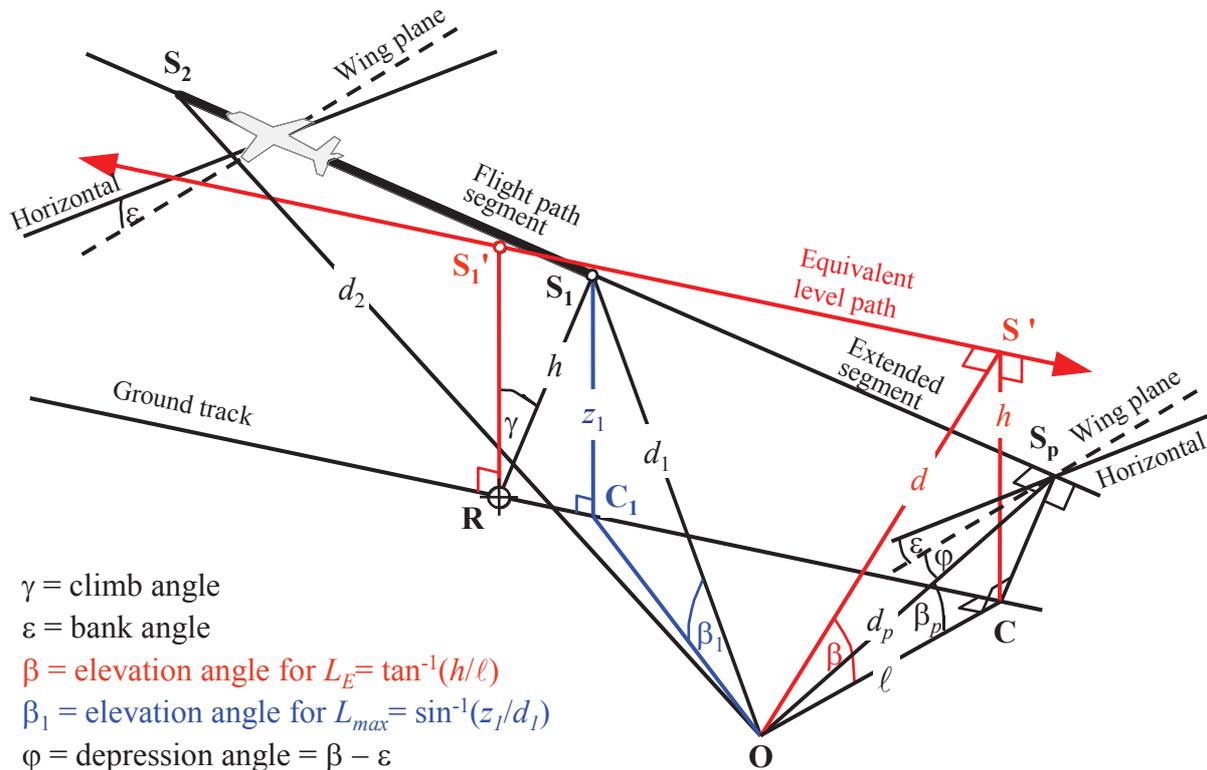
For maximum level metrics, the NPD distance parameter is taken as the shortest distance to the segment, namely $d = d_1$. For exposure level metrics, it is the shortest distance d_p from **O** to $\mathbf{S_p}$ on the extended flight path; namely the level interpolated from the NPD table is $L_{E\infty}(P_1, d_p)$.

The geometrical parameters for lateral attenuation also differ for maximum and exposure level calculations. For *maximum level* metrics the adjustment $\Lambda(\beta,\ell)$ is given by equation 2.7.40 with $\beta = \beta_1 = \sin^{-1}(z_1/d_1)$ and $\ell = OC_1 = \sqrt{d_1^2 - z_1^2}$ where β_1 and d_1 are defined by the triangle $\mathbf{OC_1S_1}$ in the vertical plane through **O** and $\mathbf{S_1}$.

When calculating the lateral attenuation for airborne segments only and *exposure level* metrics, ℓ remains the shortest lateral displacement from the segment extension (**OC**). But to define an appropriate value of β it is again necessary to visualise an (infinite) *equivalent level flight path* of which the segment can be considered part. This is drawn through $\mathbf{S_1'}$, height h above the surface, where h is equal to the length of $\mathbf{RS_1}$ the perpendicular from the ground track to the segment. This is equivalent to rotating the actual extended flight path through angle γ about point **R** (see **Figure 2.7.q**). Insofar as **R** is on the perpendicular to $\mathbf{S_1}$, the point on the segment that is closest to **O**, the construction of the equivalent level path is the same as when **O** is alongside the segment.

The closest point of approach of the equivalent level path to the observer **O** is at **S´**, slant distance d, so that the triangle **OCS´** so formed in the vertical plane then defines the elevation angle $\beta = \cos^{-1}(\ell/d)$. Although this transformation might seem rather convoluted, it should be noted that the basic source geometry (defined by d_1, d_2 and φ) remains untouched, the

sound travelling from the segment *towards* the observer is simply what it would be if the entire flight along the infinitely extended inclined segment (of which for modelling purposes the segment forms part) were at constant speed V and power P_l. The lateral attenuation of sound from the segment *received* by the observer, on the other hand, is related not to β_p, the elevation angle of the extended path, but to β, that of the equivalent level path.

Remembering that, as conceived for modelling purposes, the engine installation effect Δ_I is two-dimensional, the defining depression angle φ is still measured laterally from the aircraft wing plane (the baseline event level is still that generated by the aircraft traversing the infinite flight path represented by the extended segment). Thus the depression angle is determined at the closest point of approach, namely $\varphi = \beta_p - \varepsilon$ where β_p is angle $\mathbf{S_pOC}$.

The case of an observer ahead of the segment is not described separately; it is evident that this is essentially the same as the case of the observer behind.

However, for exposure level metrics *where observer locations are behind ground segments during the takeoff roll and ahead of ground segments during the landing roll*, the value of β becomes the same as that for maximum level metrics.

For locations behind takeoff roll segments:

$$\beta = \beta_1 = \sin^{-1}(z_1/d_1) \text{ and } \ell = OC_1 = \sqrt{d_1^2 - z_1^2}$$

For locations ahead of landing roll segments:

$$\beta = \beta_2 = \sin^{-1}(z_2/d_2) \text{ and } \ell = OC_2 = \sqrt{d_2^2 - z_2^2}$$

The rationale for using these particular expressions is related to the application of the start-of-roll directivity function behind takeoff roll segments and a semi-circular directivity assumption ahead of landing roll segments.

The finite segment correction Δ_F (Exposure levels L_E only)

The adjusted baseline noise exposure level relates to an aircraft in continuous, straight, steady level flight (albeit with a bank angle ε that is inconsistent with straight flight). Applying the (negative) *finite segment correction* $\Delta_F = 10 \cdot \lg(F)$, where F is the *energy fraction*, further adjusts the level to what it would be if the aircraft traversed the finite segment only (or were completely silent for the remainder of the infinite flight path).

The energy fraction term accounts for the pronounced longitudinal directivity of aircraft noise and the angle subtended by the segment at the observer position. Although the processes that cause the directionality are very complex, studies have shown that the resulting contours are quite insensitive to the precise directional characteristics assumed. The expression for Δ_F below is based on a fourth-power 90-degree dipole model of sound radiation. It is assumed to be unaffected by lateral directivity and attenuation. How this correction is derived is described in detail in **Appendix E**.

The energy fraction F is a function of the 'view' triangle $\mathbf{OS_1S_2}$ defined in **Figures 2.7.j to 2.7.l** such that:

$\Delta_F = 10 \cdot \log\left[\frac{1}{\pi}\left(\frac{\alpha_2}{1+\alpha_2^2} + arctan\alpha_2 - \frac{\alpha_1}{1+\alpha_1^2} - arctan\alpha_1\right)\right]$	(2.7.45)

with

$$\alpha_1 = -\frac{q}{d_\lambda} \; ; \quad \alpha_2 = -\frac{q-\lambda}{d_\lambda} \; ; \quad d_\lambda = d_0 \cdot 10^{[L_{E\infty}(P,d_p)-L_{max}(P,d_p)]/10} \; ; \quad d_0 = \frac{2}{\pi} \cdot V_{ref} \cdot t_0.$$

where d_λ is known as the 'scaled distance' (see **Appendix E**) and V_{ref} = 270.05 ft/s (for the 160 knots reference speed). Note that $L_{max}(P, d_p)$ is the maximum level, from NPD data, for perpendicular distance d_p, NOT the segment L_{max}. It is advised to apply a lower limit of -150 dB to Δ_F.

In the particular case of observer locations behind every takeoff ground-roll segment, a reduced form of the noise fraction expressed in Equation 2.7.45 is used, which corresponds to the specific case of q = 0.

This is denoted $\Delta'_{F,d}$ where 'd' clarifies its use for departure operations, and is computed as:

$$\Delta'_{F,d} = 10 \cdot log_{10}\left[\frac{1}{\pi}\left(\frac{\alpha_2}{1+\alpha_2^2} + arctan\alpha_2\right)\right]$$	(2.7.46.a)

where $\alpha_2 = \lambda / d_\lambda$.

This particular form of the noise fraction is used in conjunction with the start-of-roll directivity function, whose application method is further explained in the section below.

In the particular case of observer locations ahead of <u>every</u> landing ground-roll segment, a reduced form of the noise fraction expressed in equation 2.7.45 is used, which corresponds to the specific case of q = λ. This is denoted $\Delta'_{F,a}$ where 'a' clarifies its use for arrival operations, and is computed as:

$$\Delta'_{F,a} = 10 \cdot log_{10}\left[\frac{1}{\pi}\left(-\frac{\alpha_1}{1+\alpha_1^2} - arctan\alpha_1\right)\right]$$	(2.7.46.b)

where $\alpha_1 = -\lambda / d_\lambda$.

The use of this form, without the application of any further horizontal directivity adjustment (unlike the case of locations behind takeoff ground-roll segments – see section on start-of-roll directivity), implicitly assumes a semi-circular horizontal directivity ahead of landing ground roll segments.

The start-of-roll directivity function Δ_{SOR}

The noise of aircraft – especially jet aircraft equipped with lower by-pass ratio engines – exhibits a lobed radiation pattern in the rearward arc, which is characteristic of jet exhaust noise. This pattern is the more pronounced the higher the jet velocity and the lower the aircraft speed. This is of special significance for observer locations behind the start of roll, where both conditions are fulfilled. This effect is taken into account by a directivity function Δ_{SOR}.

The function Δ_{SOR} has been derived from several noise measurement campaigns using microphones adequately positioned behind and on the side of the SOR of departing jet aircraft.

Figure 2.7.r shows the relevant geometry. The azimuth angle Ψ between the aircraft longitudinal axis and the vector to the observer is defined by

$\psi = arccos\left(\dfrac{q}{d_{SOR}}\right).$	(2.7.47)

The relative distance q is negative (see **Figure 2.7.j**) so that Ψ ranges from 90° relative to the aircraft forward heading, to 180° in the reverse direction.

Figure 2.7.r

Aircraft-observer geometry for estimation of directivity correction
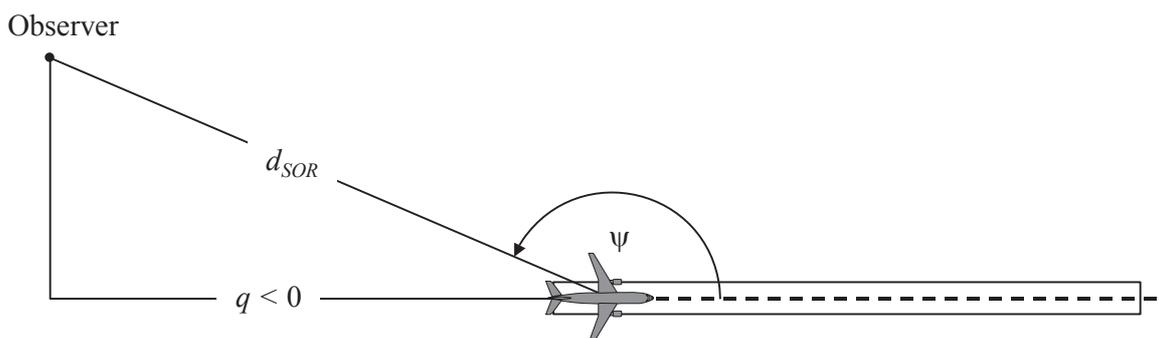
The function Δ_{SOR} represents the variation of the overall noise emanating from the takeoff ground roll measured behind the start of roll, relatively to the overall noise from takeoff ground roll measured on the side of the SOR, at the same distance:

$$L_{TGR}(d_{SOR}, \psi) = L_{TGR}(d_{SOR}, 90°) + \Delta_{SOR}(d_{SOR}, \psi) \qquad (2.7.48)$$

where $L_{TGR}(d_{SOR}, 90°)$ is the overall takeoff ground roll noise level at the point distance d_{SOR} to the side of the SOR. Δ_{SOR} is implemented as an adjustment to the noise level from one flight path segment (e.g. $L_{max,seg}$ or $L_{E,seg}$), as described in equation 2.7.28.

The SOR directivity function, in decibels, for *turbofan-powered jet aircraft* is given by the following equation:

For 90° ≤ Ψ < 180° then:

$\Delta^0_{SOR} = 2329.44 - (8.0573 \cdot \psi) +$ $\left(11.51 \cdot exp\left(\dfrac{\pi \cdot \psi}{180}\right)\right) - \left(\dfrac{3.4601 \cdot \psi}{ln\left(\dfrac{\pi \cdot \psi}{180}\right)}\right) -$ $\left(\dfrac{17403338.3 \cdot ln\left(\dfrac{\pi \cdot \psi}{180}\right)}{\psi^2}\right)$	(2.7.49)

The SOR directivity function, in decibels, for *turboprop-powered aircraft* is given by the following equation:

For 90° ≤ Ψ < 180° then:

$$\begin{aligned} \Delta_{SOR}^0 &= -34643.898 + \left(\frac{30722161.987}{\psi}\right) \\ &- \left(\frac{11491573930.510}{\psi^2}\right) \\ &+ \left(\frac{2349285669062}{\psi^3}\right) \\ &- \left(\frac{283584441904272}{\psi^4}\right) \\ &+ \left(\frac{20227150391251300}{\psi^5}\right) \\ &- \left(\frac{790084471305203000}{\psi^6}\right) \\ &+ \left(\frac{13050687178273800000}{\psi^7}\right) \end{aligned}$$	(2.7.50)

If the distance d_{SOR} exceeds the normalising distance $d_{SOR,0}$, the directivity correction is multiplied by a correction factor to account for the fact that the directivity becomes less pronounced for greater distances from the aircraft; namely

$\Delta_{SOR} = \Delta_{SOR}^0 \quad \text{if} \quad d_{SOR} \leq d_{SOR,0}$	(2.7.51)
$\Delta_{SOR} = \Delta_{SOR}^0 \cdot \dfrac{d_{SOR,0}}{d_{SOR}} \quad \text{if} \quad d_{SOR} > d_{SOR,0}$	(2.7.52)

The normalising distance $d_{SOR,0}$ equals 762 m (2500 ft).

The Δ_{SOR} function described above mostly captures the pronounced directivity effect of the initial portion of the takeoff roll at locations behind the SOR (because it is the closest to the receivers, with the highest jet velocity to aircraft speed ratio). However, the use of the hence established Δ_{SOR} is 'generalised' to positions behind *each* individual takeoff ground roll segment, so not only behind the start-of-roll point (in the case of takeoff). *The established Δ_{SOR} is not applied to positions ahead of individual takeoff ground roll segments, nor is it applied to positions behind or ahead of individual landing ground roll segments*.

The parameters d_{SOR} and Ψ are calculated relative to the start of each individual ground roll segment. The event level L_{SEG} for a location behind a given takeoff ground-roll segment is calculated to comply with the formalism of the Δ_{SOR} function: it is essentially calculated for the reference point located on the side of the start point of the segment, at the same distance d_{SOR} as the actual point, and is further adjusted with Δ_{SOR} to obtain the event level at the actual point.

Note: Formulas (2.7.53), (2.7.54) and (2.7.55) were removed in the latest amendment of this Annex.'

(17)   Section 2.8 is replaced by the following:

'2.8 Exposure to noise

Determination of the area exposed to noise

The assessment of the area exposed to noise is based on noise assessment points at 4 m ± 0,2 above the ground, corresponding to the receiver points as defined in 2.5, 2.6 and 2.7, calculated on a grid for individual sources.

Grid points that are located inside buildings shall be assigned a noise level result by assigning the quietest nearby noise receiver points outside buildings, except for aircraft noise where the calculation is performed without considering the presence of buildings and in which case the noise receiver point falling within a building is directly used.

Depending on the grid resolution, the corresponding area is assigned to each calculation point in the grid. For example, with a 10 m x 10 m grid, each assessment point represents an area of 100 square metres that is exposed to the calculated noise level.

Assigning noise assessment points to buildings not containing dwellings

The assessment of the exposure of buildings not containing dwellings such as schools and hospitals to noise is based on noise assessment points at 4 ± 0,2 m above the ground, corresponding to the receiver points as defined in 2.5, 2.6 and 2.7

For the assessment of buildings not containing dwellings and exposed to aircraft noise, each building is associated to the noisiest noise receiver point falling within the building itself or, if not present, on the grid surrounding the building.

For the assessment of buildings not containing dwellings and exposed to land-based noise sources, receiver points are placed at approximately 0,1 m in front of building façades. Reflections from the façade being considered shall be excluded from the calculation. The building is then associated to the noisiest receiver point on its façades.

Determination of the dwellings and people living in dwellings exposed to noise

For the assessment of the noise exposure of dwellings and the exposure of people living in dwellings, only residential buildings shall be considered. No dwellings or people shall be assigned to other buildings without residential use such as buildings exclusively used as schools, hospitals, office buildings or factories. The assignment of the dwellings, and people living in dwellings, to the residential buildings shall be based on the latest official data (depending on the Member State's relevant regulations).

The number of dwellings, and people living in dwellings, in residential buildings are important intermediate parameters for the estimation of the exposure to noise. Unfortunately, data on these parameters is not always available. Below, it is specified how these parameters can be derived from data more readily available.

Symbols used in the following are:

BA = base area of the building

DFS = dwelling floor space

DUFS = dwelling unit floor space

H = height of the building

FSI = dwelling floor space per person living in dwellings

Dw = number of dwellings

Inh = number of people living in dwellings

NF = number of floors

V = volume of residential buildings

For the calculation of the number of dwellings, and people living in dwellings, either the following Case 1 procedure or the Case 2 procedure shall be used, depending on the availability of data.

Case 1: the data on the number of dwellings and people living in dwellings is available

1A:

The number of people living in dwellings is known or has been estimated on the basis of the number of dwelling units. In this case the number of people living in dwellings for a building is the sum of the number of people living in all dwelling units in the building:

$$Inh_{building} = \sum_{i=1}^{n} Inh_{dwelling_{unit_i}}$$	(2.8.1)

1B:

The number of dwellings or people living in dwellings is only known for entities larger than a building, e.g., enumeration areas, city blocks, districts or even an entire municipality. In this case the number of dwellings, and people living in dwellings, in a building is estimated based on the volume of the building:

$$Dw_{building} = \frac{V_{building}}{V_{total}} \times Dw_{total}$$	(2.8.2a)

$$Inh_{building} = \frac{V_{building}}{V_{total}} \times Inh_{total}$$	(2.8.2b)

The index ´total´ here refers to the respective entity considered. The volume of the building is the product of its base area and its height:

$$V_{building} = BA_{building} \times H_{building}$$	(2.8.3)

If the height of the building is not known, it shall be estimated based on the number of floors $NF_{building}$, assuming an average height per floor of 3 m:

$$H_{building} = NF_{building} \times 3m$$	(2.8.4)

If the number of floors is also not known, a default value for the number of floors, representative of the district or the borough, shall be used. The total volume of residential buildings in the entity considered V_{total} is calculated as the sum of the volumes of all residential buildings in the entity:

(2.8.5)

$$V_{total} = \sum_{i=1}^{n} V_{building_i}$$	(2.8.5)

Case 2: no data on the number of people living in dwellings is available

In this case, the number of people living in dwellings is estimated based on the average dwelling floor space per person living in dwellings FSI. If this parameter is not known, a default value shall be used.

2A:

The dwelling floor space is known on the basis of dwelling units.

In this case the number of people living in each dwelling unit is estimated as follows:

$$Inh_{dwelling_{unit_i}} = \frac{DUFS_i}{FSI}$$	(2.8.6)

The total number of people living in dwellings for the building can now be estimated as in Case 1A.

2B:

The dwelling floor space is known for the entire building, that is to say, the sum of the dwelling floor spaces of all dwelling units in the building is known.

In this case the number of people living in dwellings is estimated as follows:

$$Inh_{building} = \frac{DFS_{building}}{FSI}$$	(2.8.7)

2C:

The dwelling floor space is known only for entities larger than a building, e.g., enumeration areas, city blocks, districts or even an entire municipality.

In this case the number of people living in dwellings for a building is estimated based on the volume of the building as described in Case 1B with the total number of people living in dwellings estimated as follows:

$$Inh_{total} = \frac{DFS_{total}}{FSI}$$	(2.8.8)

2D:

The dwelling floor space is unknown.

In this case the number of people living in dwellings for a building is estimated as described in Case 2B with the dwelling floor space estimated as follows:

(2.8.9)

$$DFS_{building} = BA_{building} \times 0.8 \times NF_{building}$$	(2.8.9)

The factor 0.8 is the conversion factor *gross floor area → dwelling floor space*. If a different factor is known to be representative of the area it shall be used instead and clearly documented. If the number of floors of the building is not known, it shall be estimated based

on the height of the building, $H_{building}$, which typically results in a non-integer number of floors:

$$NF_{building} = \dfrac{H_{building}}{3\text{m}}$$	(2.8.10)

If neither the height of the building nor the number of floors is known, a default value for the number of floors, representative of the district or the borough, shall be used.

Assigning noise assessment points to dwellings and people living in dwellings

The assessment of the exposure of dwellings, and people living in dwellings, to noise is based on noise assessment points at 4 ± 0,2 m above the ground, corresponding to the receiver points as defined in 2.5, 2.6 and 2.7.

For the calculation of the number of dwellings, and people living in dwellings for aircraft noise, all dwellings, and people living in dwellings, within a building are associated to the noisiest noise receiver point falling within the building itself or, if not present, on the grid surrounding the building.

For the calculation of the number of dwellings, and people living in dwellings for land-based noise sources, receiver points are placed at approximately 0,1 m in front of building façades of residential buildings. Reflections from the façade being considered shall be excluded from the calculation. Either the following Case 1 procedure or the Case 2 procedure shall be used to locate the receiver points.

Case 1: façades split up in regular intervals on each façade

Figure 2.8.a

Example of location of receiver points around a building following Case 1 procedure
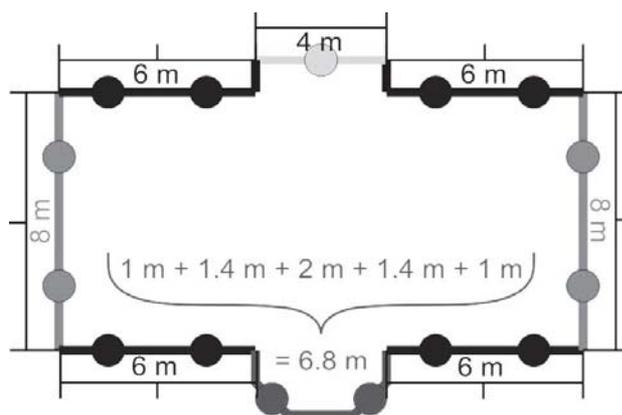
(a) Segments of a length of more than 5 m are split up into regular intervals of the longest possible length but less than or equal to 5 m. Receiver points are placed in the middle of each regular interval.

(b) Remaining segments above a length of 2.5 m are represented by one receiver point in the middle of each segment.

(c) Remaining adjacent segments with a total length of more than 5 m are treated as polyline objects in a manner similar to that described in a) and b).

Case 2: façades split up at set distance from start of polygon

Figure 2.8.b

Example of location of receiver points around a building following Case 2 procedure
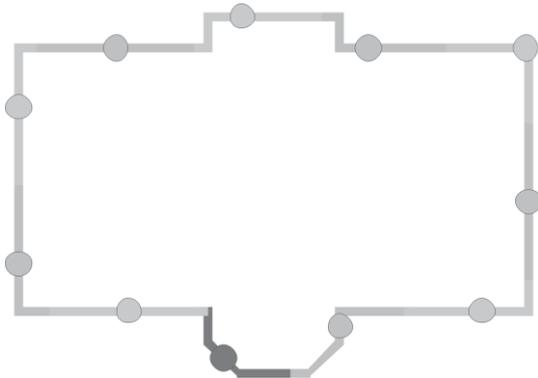
(a) Façades are considered separately or are split up every 5 m from the start position onwards, with a receiver position placed at the halfway distance of the façade or the 5m segment

(b) The remaining section has its receiver point in its mid-point.

Assigning dwellings and people living in dwellings to receiver points

Where information on the location of dwellings within building footprints is available, that dwelling and the people living in that dwelling are assigned to the receiver point at the most exposed façade of that dwelling. For example, for detached houses, for semi-detached and terrace houses, or apartment buildings, where the internal division of the building is known, or for buildings with a floor size that indicates a single dwelling per floor level, or for buildings with a floor size and height that indicates a single dwelling per building.

Where no information on the location of dwellings within building footprints as explained above is available, one of the two following methods shall be used, as appropriate, on a building by building basis to estimate the exposure to noise of the dwellings and people in dwellings within the buildings.

a) Available information shows that dwellings are arranged within an apartment building such that they have a single façade exposed to noise

In this case, the allocation of the number of dwellings, and people living in dwellings, to receiver points, shall be weighted by the length of the represented façade according to the procedure under either Case 1 or Case 2, so that the sum of all receiver points represents the total number of dwellings and people living in dwellings assigned to the building.

b) Available information shows that dwellings are arranged within an apartment building such that they have more than one façade exposed to noise, or no information is available on how many facades of the dwellings are exposed to noise.

In this case, for each building, the set of associated receiver locations shall be split into a lower and upper half based on the median[7] value of the calculated assessment levels for each building. In case of odd number of receiver points, the procedure is applied excluding the receiver location with the lowest noise level.

For each receiver point in the upper half of the data set, the number of dwellings, and people living in dwellings, shall be distributed equally, so that the sum of all receiver points in the upper half of the data set represents the total number of dwellings and people living in dwellings. No dwellings or people living in dwellings will be assigned to receivers in the lower half of the data set[8].'

(18) Appendix D is amended as follows:

(a) the first sub-paragraph under Table D-1 is replaced by the following:

'The attenuation coefficients in **Table D-1** may be assumed valid over reasonable ranges of temperature and humidity. However, to check whether adjustments may be necessary, SAE ARP-5534 should be used to calculate average atmospheric absorption coefficients for the average airport temperature *T* and relative humidity *RH*. Where, from a comparison of these with those in **Table D-1**, it is judged that adjustment is required the following methodology should be used. '

(b) in the third sub-paragraph under Table D-1, points 2 and 3 are replaced by the following:

'2. Next the corrected spectrum is adjusted to each of the ten standard NPD distances d_i using attenuation rates for both (i) the SAE AIR-1845 atmosphere and (ii) the user-specified atmosphere (based on SAE ARP-5534).

(i) For the SAE AIR-1845 atmosphere:

$L_{n,ref}(d_i) = L_n(d_{ref}) - 20.\lg(d_i/d_{ref}) - \alpha_{n,ref} \cdot d_i$	(D-2)

(ii) For the user-specified atmosphere:

$L_{n,5534}(T,RH,d_i) = L_n(d_{ref}) - 20.\lg(d_i/d_{ref}) -$ $\alpha_{n,5534}(T,RH) \cdot d_i$	(D-3)

where $\alpha_{n,5534}$ is the coefficient of atmospheric absorption for the frequency band *n* (expressed in dB/m) calculated using SAE ARP-5534 with temperature *T*, and relative humidity *RH*.

3. At each NPD distance d_i the two spectra are A-weighted and decibel-summed to determine the resulting A-weighted levels $L_{A,5534}$ and $L_{A,ref}$ - which are then subtracted arithmetically:

---

[7] The medium value is the value separating the higher half (50%) from the lower half (50%) of a data set.
[8] The lower half of the data asset may be assimilated with the presence of relatively calm façades. In case it is known in advance, e.g. based on the location of buildings relative to the dominant noise sources, which receiver locations will give way to the highest / lowest noise levels, there is no need to calculate noise for the lower half.

$\Delta L(T, RH, d_i) = L_{A,5534} - L_{A,ref} = 10 \cdot lg \sum_{n=1}^{24} 10^{(L_{n,5534}(T,RH,d_i)-A_n)/10} - 10 \cdot lg \sum_{n=1}^{24} 10^{(L_{n,ref}(d_i)-A_n)/10}$									(D-4)

,

(19)   Appendix F is amended as follows:

(a)   Table F-1 is replaced by the following:

'

Category	Coefficient	63	125	250	500	1000	2000	4000	8000
1	A_R	83.1	89.2	87.7	93.1	100.1	96.7	86.8	76.2
	B_R	30.0	41.5	38.9	25.7	32.5	37.2	39.0	40.0
	A_P	97.9	92.5	90.7	87.2	84.7	88.0	84.4	77.1
	B_P	-1.3	7.2	7.7	8.0	8.0	8.0	8.0	8.0
2	A_R	88.7	93.2	95.7	100.9	101.7	95.1	87.8	83.6
	B_R	30.0	35.8	32.6	23.8	30.1	36.2	38.3	40.1
	A_P	105.5	100.2	100.5	98.7	101.0	97.8	91.2	85.0
	B_P	-1.9	4.7	6.4	6.5	6.5	6.5	6.5	6.5
3	A_R	91.7	96.2	98.2	104.9	105.1	98.5	91.1	85.6
	B_R	30.0	33.5	31.3	25.4	31.8	37.1	38.6	40.6
	A_P	108.8	104.2	103.5	102.9	102.6	98.5	93.8	87.5
	B_P	0.0	3.0	4.6	5.0	5.0	5.0	5.0	5.0
4a	A_R	0.0	0.0	0.0	0.0	0.0	0.0	0.0	0.0
	B_R	0.0	0.0	0.0	0.0	0.0	0.0	0.0	0.0
	A_P	93,0	93,0	93,5	95,3	97,2	100,4	95,8	90,9
	B_P	4,2	7,4	9,8	11,6	15,7	18,9	20,3	20,6
4b	A_R	0.0	0.0	0.0	0.0	0.0	0.0	0.0	0.0
	B_R	0.0	0.0	0.0	0.0	0.0	0.0	0.0	0.0

	A_P	99,9	101,9	96,7	94,4	95,2	94,7	92,1	88,6
	B_P	3,2	5,9	11,9	11,6	11,5	12,6	11,1	12,0
5	A_R								
	B_R								
	A_P								
	B_P								

’

(b)   Table F-4 is replaced by the following:

'

Description	Min speed at which it is valid [km/h]	Maximum speed at which it is valid [km/h]	Cate-gory	α_m (63 Hz)	α_m (125 Hz)	α_m (250 Hz)	α_m (500 Hz)	α_m (1 kHz)	α_m (2 kHz)	α_m (4 kHz)	α_m (8 kHz)	β_m
Reference road surface	--	--	1	0,0	0,0	0,0	0,0	0,0	0,0	0,0	0,0	0,0
			2	0,0	0,0	0,0	0,0	0,0	0,0	0,0	0,0	0,0
			3	0,0	0,0	0,0	0,0	0,0	0,0	0,0	0,0	0,0
			4a/4b	0,0	0,0	0,0	0,0	0,0	0,0	0,0	0,0	0,0
1-layer ZOAB	50	130	1	0,0	5,4	4,3	4,2	-1,0	-3,2	-2,6	0,8	-6,5
			2	7,9	4,3	5,3	-0,4	-5,2	-4,6	-3,0	-1,4	0,2
			3	9,3	5,0	5,5	-0,4	-5,2	-4,6	-3,0	-1,4	0,2
			4a/4b	0,0	0,0	0,0	0,0	0,0	0,0	0,0	0,0	0,0
2-layer ZOAB	50	130	1	1,6	4,0	0,3	-3,0	-4,0	-6,2	-4,8	-2,0	-3,0
			2	7,3	2,0	-0,3	-5,2	-6,1	-6,0	-4,4	-3,5	4,7
			3	8,3	2,2	-0,4	-5,2	-6,2	-6,1	-4,5	-3,5	4,7
			4a/4b	0,0	0,0	0,0	0,0	0,0	0,0	0,0	0,0	0,0
2-layer ZOAB (fine)	80	130	1	-1,0	3,0	-1,5	-5,3	-6,3	-8,5	-5,3	-2,4	-0,1
			2	7,9	0,1	-1,9	-5,9	-6,1	-6,8	-4,9	-3,8	-0,8
			3	9,4	0,2	-1,9	-5,9	-6,1	-6,7	-4,8	-3,8	-0,9
			4a/4b	0,0	0,0	0,0	0,0	0,0	0,0	0,0	0,0	0,0
SMA-NL5	40	80	1	10,3	-0,9	0,9	1,8	-1,8	-2,7	-2,0	-1,3	-1,6
			2	0,0	0,0	0,0	0,0	0,0	0,0	0,0	0,0	0,0
			3	0,0	0,0	0,0	0,0	0,0	0,0	0,0	0,0	0,0
			4a/4b	0,0	0,0	0,0	0,0	0,0	0,0	0,0	0,0	0,0

SMA-NL8	40	80	1	6,0	0,3	0,3	0,0	-0,6	-1,2	-0,7	-0,7	-1,4
			2	0,0	0,0	0,0	0,0	0,0	0,0	0,0	0,0	0,0
			3	0,0	0,0	0,0	0,0	0,0	0,0	0,0	0,0	0,0
			4a/4b	0,0	0,0	0,0	0,0	0,0	0,0	0,0	0,0	0,0
Brushed down concrete	70	120	1	8,2	-0,4	2,8	2,7	2,5	0,8	-0,3	-0,1	1,4
			2	0,3	4,5	2,5	-0,2	-0,1	-0,5	-0,9	-0,8	5,0
			3	0,2	5,3	2,5	-0,2	-0,1	-0,6	-1,0	-0,9	5,5
			4a/4b	0,0	0,0	0,0	0,0	0,0	0,0	0,0	0,0	0,0
Optimised brushed down concrete	70	80	1	-0,2	-0,7	1,4	1,2	1,1	-1,6	-2,0	-1,8	1,0
			2	-0,7	3,0	-2,0	-1,4	-1,8	-2,7	-2,0	-1,9	-6,6
			3	-0,5	4,2	-1,9	-1,3	-1,7	-2,5	-1,8	-1,8	-6,6
			4a/4b	0,0	0,0	0,0	0,0	0,0	0,0	0,0	0,0	0,0
Fine broomed concrete	70	120	1	8,0	-0,7	4,8	2,2	1,2	2,6	1,5	-0,6	7,6
			2	0,2	8,6	7,1	3,2	3,6	3,1	0,7	0,1	3,2
			3	0,1	9,8	7,4	3,2	3,1	2,4	0,4	0,0	2,0
			4a/4b	0,0	0,0	0,0	0,0	0,0	0,0	0,0	0,0	0,0
Worked surface	50	130	1	8,3	2,3	5,1	4,8	4,1	0,1	-1,0	-0,8	-0,3
			2	0,1	6,3	5,8	1,8	-0,6	-2,0	-1,8	-1,6	1,7
			3	0,0	7,4	6,2	1,8	-0,7	-2,1	-1,9	-1,7	1,4
			4a/4b	0,0	0,0	0,0	0,0	0,0	0,0	0,0	0,0	0,0
Hard elements in herring-bone	30	60	1	27,0	16,2	14,7	6,1	3,0	-1,0	1,2	4,5	2,5
			2	29,5	20,0	17,6	8,0	6,2	-1,0	3,1	5,2	2,5
			3	29,4	21,2	18,2	8,4	5,6	-1,0	3,0	5,8	2,5
			4a/4b	0,0	0,0	0,0	0,0	0,0	0,0	0,0	0,0	0,0
Hard elements not in herring-bone	30	60	1	31,4	19,7	16,8	8,4	7,2	3,3	7,8	9,1	2,9
			2	34,0	23,6	19,8	10,5	11,7	8,2	12,2	10,0	2,9
			3	33,8	24,7	20,4	10,9	10,9	6,8	12,0	10,8	2,9

			4a/4b	0,0	0,0	0,0	0,0	0,0	0,0	0,0	0,0	0,0
Quiet hard elements	30	60	1	26,8	13,7	11,9	3,9	-1,8	-5,8	-2,7	0,2	-1,7
			2	9,2	5,7	4,8	2,3	4,4	5,1	5,4	0,9	0,0
			3	9,1	6,6	5,2	2,6	3,9	3,9	5,2	1,1	0,0
			4a/4b	0,0	0,0	0,0	0,0	0,0	0,0	0,0	0,0	0,0
Thin layer A	40	130	1	10,4	0,7	-0,6	-1,2	-3,0	-4,8	-3,4	-1,4	-2,9
			2	13,8	5,4	3,9	-0,4	-1,8	-2,1	-0,7	-0,2	0,5
			3	14,1	6,1	4,1	-0,4	-1,8	-2,1	-0,7	-0,2	0,3
			4a/4b	0,0	0,0	0,0	0,0	0,0	0,0	0,0	0,0	0,0
Thin layer B	40	130	1	6,8	-1,2	-1,2	-0,3	-4,9	-7,0	-4,8	-3,2	-1,8
			2	13,8	5,4	3,9	-0,4	-1,8	-2,1	-0,7	-0,2	0,5
			3	14,1	6,1	4,1	-0,4	-1,8	-2,1	-0,7	-0,2	0,3
			4a/4b	0,0	0,0	0,0	0,0	0,0	0,0	0,0	0,0	0,0

'

(20)   Appendix G is amended as follows:

(a)   in Table G-1, the second table is replaced by the following:

'

$L_{r,TR,i}$		
Wavelength	Rail Roughness	
	E	M
	EN ISO 3095:2013 (Well maintained and very smooth)	Average network (Normally maintained smooth)
2 000 mm	17,1	35,0
1 600 mm	17,1	31,0
1 250 mm	17,1	28,0
1 000 mm	17,1	25,0
800 mm	17,1	23,0

630 mm	17,1	20,0
500 mm	17,1	17,0
400 mm	17,1	13,5
315 mm	15,0	10,5
250 mm	13,0	9,0
200 mm	11,0	6,5
160 mm	9,0	5,5
125 mm	7,0	5,0
100 mm	4,9	3,5
80 mm	2,9	2,0
63 mm	0,9	0,1
50 mm	−1,1	-0,2
40 mm	−3,2	-0,3
31,5 mm	−5,0	-0,8
25 mm	−5,6	-3,0
20 mm	−6,2	-5,0
16 mm	−6,8	-7,0
12,5 mm	−7,4	-8,0
10 mm	−8,0	-9,0
8 mm	−8,6	-10,0
6,3 mm	−9,2	-12,0
5 mm	−9,8	-13,0
4 mm	−10,4	-14,0
3,15 mm	−11,0	-15,0
2,5 mm	−11,6	-16,0
2 mm	−12,2	-17,0

1,6 mm	−12,8	-18,0
1,25 mm	−13,4	-19,0
1 mm	−14,0	-19,0
0,8 mm	−14,0	-19,0

'

(b)   Table G-2 is replaced by the following:

'

$A_{3,i}$					
1.1. **Wavelength**	Wheel load 50 kN - wheel diameter 360 mm	Wheel load 50 kN - wheel diameter 680 mm	Wheel load 50 kN - wheel diameter 920 mm	Wheel load 25 kN - wheel diameter 920 mm	Wheel load 100 kN - wheel diameter 920 mm
2 000 mm	0,0	0,0	0,0	0,0	0,0
1 600 mm	0,0	0,0	0,0	0,0	0,0
1 250 mm	0,0	0,0	0,0	0,0	0,0
1 000 mm	0,0	0,0	0,0	0,0	0,0
800 mm	0,0	0,0	0,0	0,0	0,0
630 mm	0,0	0,0	0,0	0,0	0,0
500 mm	0,0	0,0	0,0	0,0	0,0
400 mm	0,0	0,0	0,0	0,0	0,0
315 mm	0,0	0,0	0,0	0,0	0,0
250 mm	0,0	0,0	0,0	0,0	0,0
200 mm	0,0	0,0	0,0	0,0	0,0
160 mm	0,0	0,0	0,0	0,0	-0,1
125 mm	0,0	0,0	-0,1	0,0	-0,2
100 mm	0,0	-0,1	-0,1	0,0	-0,3
80 mm	-0,1	-0,2	-0,3	-0,1	-0,6

63 mm	-0,2	-0,3	-0,6	-0,3	-1,0
50 mm	-0,3	-0,7	-1,1	-0,5	-1,8
40 mm	-0,6	-1,2	-1,3	-1,1	-3,2
31,5 mm	-1,0	-2,0	-3,5	-1,8	-5,4
25 mm	-1,8	-4,1	-5,3	-3,3	-8,7
20 mm	-3,2	-6,0	-8,0	-5,3	-12,2
16 mm	-5,4	-9,2	-12,0	-7,9	-16,7
12,5 mm	-8,7	-13,8	-16,8	-12,8	-17,7
10 mm	-12,2	-17,2	-17,7	-16,8	-17,8
8 mm	-16,7	-17,7	-18,0	-17,7	-20,7
6,3 mm	-17,7	-18,6	-21,5	-18,2	-22,1
5 mm	-17,8	-21,5	-21,8	-20,5	-22,8
4 mm	-20,7	-22,3	-22,8	-22,0	-24,0
3,15 mm	-22,1	-23,1	-24,0	-22,8	-24,5
2,5 mm	-22,8	-24,4	-24,5	-24,2	-24,7
2 mm	-24,0	-24,5	-25,0	-24,5	-27,0
1,6 mm	-24,5	-25,0	-27,3	-25,0	-27,8
1,25 mm	-24,7	-28,0	-28,1	-27,4	-28,6
1 mm	-27,0	-28,8	-28,9	-28,2	-29,4
0.8 mm	-27,8	-29,6	-29,7	-29,0	-30,2

'

(c)   the   first   table   of   table   G-3   is   replaced   by   the   following:
'

$L_{H,TR,i}$							
Frequency	Track base / Rail pad type						
	M/S	M/M	M/H	B/S	B/M	B/H	W	D

	Mono-block sleeper on soft rail pad	Mono-block sleeper on medium stiffness rail pad	Mono-block on hard rail pad	Bi-block sleeper on soft rail pad	Bi-block sleeper on medium stiffness rail pad	Bi-block sleeper on hard rail pad	Wooden sleepers	Direct fastening on bridges
50 Hz	53,3	50,9	50,1	50,9	50,0	49,8	44,0	75,4
63 Hz	59,3	57,8	57,2	56,6	56,1	55,9	51,0	77,4
80 Hz	67,2	66,5	66,3	64,3	64,1	64,0	59,9	81,4
100 Hz	75,9	76,8	77,2	72,3	72,5	72,5	70,8	87,1
125 Hz	79,2	80,9	81,6	75,4	75,8	75,9	75,1	88,0
160 Hz	81,8	83,3	84,0	78,5	79,1	79,4	76,9	89,7
200 Hz	84,2	85,8	86,5	81,8	83,6	84,4	77,2	83,4
250 Hz	88,6	90,0	90,7	86,6	88,7	89,7	80,9	87,7
315 Hz	91,0	91,6	92,1	89,1	89,6	90,2	85,3	89,8
400 Hz	94,5	93,9	94,3	91,9	89,7	90,2	92,5	97,5
500 Hz	97,0	95,6	95,8	94,5	90,6	90,8	97,0	99,0
630 Hz	99,2	97,4	97,0	97,5	93,8	93,1	98,7	100,8
800 Hz	104,0	101,7	100,3	104,0	100,6	97,9	102,8	104,9
1000 Hz	107,1	104,4	102,5	107,9	104,7	101,1	105,4	111,8
1250 Hz	108,3	106,0	104,2	108,9	106,3	103,4	106,5	113,9
1600 Hz	108,5	106,8	105,4	108,8	107,1	105,4	106,4	115,5
2000 Hz	109,7	108,3	107,1	109,8	108,8	107,7	107,5	114,9
2500 Hz	110,0	108,9	107,9	110,2	109,3	108,5	108,1	118,2
3150 Hz	110,0	109,1	108,2	110,1	109,4	108,7	108,4	118,3
4000 Hz	110,0	109,4	108,7	110,1	109,7	109,1	108,7	118,4
5000 Hz	110,3	109,9	109,4	110,3	110,0	109,6	109,1	118,9
6300 Hz	110,0	109,9	109,7	109,9	109,8	109,6	109,1	117,5

8000 Hz	110,1	110,3	110,4	110,0	110,0	109,9	109,5	117,9
10000 Hz	110,6	111,0	111,4	110,4	110,5	110,6	110,2	118,6

'

(d)   Table G-3 is amended as follows:

–   in column 1 of section "$L_{H,\,VEH,\,i}$":
the 11th row is replaced by the following: '315 Hz';
the 21st row is replaced by the following: '3150 Hz';
the 24st row is replaced by the following: '6300 Hz'.

–   in column 1 of section "$L_{H,\,VEH,\,SUP,\,i}$":
the 11th row is replaced by the following: '315 Hz';
the 21th row is replaced by the following: '3150 Hz';
the 24th row is replaced by the following: '6300 Hz'.

(e)   Table G-4 is replaced by the following:

'

$L_{R,IMPACT,i}$	
Wavelength	Single switch/joint/crossing/100 m
2 000 mm	22,0
1 600 mm	22,0
1 250 mm	22,0
1 000 mm	22,0
800 mm	22,0
630 mm	20,0
500 mm	16,0
400 mm	15,0
315 mm	14,0
250 mm	15,0

200 mm	14,0
160 mm	12,0
125 mm	11,0
100 mm	10,0
80 mm	9,0
63 mm	8,0
50 mm	6,0
40 mm	3,0
31,5 mm	2,0
25 mm	-3,0
20 mm	-8,0
16 mm	-13,0
12,5 mm	-17,0
10 mm	-19,0
8 mm	-22,0
6,3 mm	-25,0
5 mm	-26,0
4 mm	-32,0
3,15 mm	-35,0
2,5 mm	-40,0
2 mm	-43,0
1,6 mm	-45,0
1,25 mm	-47,0
1 mm	-49,0
0,8 mm	-50,0

'

(f)   in Table G-5:

the 1st column, 12th row is replaced by the following: '315 Hz';

the 1st column, 22nd row is replaced by the following: '3150 Hz';

the 1st column, 25th row is replaced by the following: '6300 Hz';

the 4th column, 25th row is replaced by the following: '81,4';

the 5th column, 25th row is replaced by the following: '80,7'.

(g)   in Table G-6, in column 1:

The 11th row is replaced by the following: '315 Hz';

The 21rd row is replaced by the following: '3150 Hz';

The 24th row is replaced by the following: '6300 Hz'.

(h)   Table G-7 is replaced by the following:

'

$L_{H,\text{bridge},i}$		
Frequency	+10 dB(A)	+15 dB(A)
50 Hz	85,2	90,1
63 Hz	87,1	92,1
80 Hz	91,0	96,0
100 Hz	94,0	99,5
125 Hz	94,4	99,9
160 Hz	96,0	101,5
200 Hz	92,5	99,6
250 Hz	96,7	103,8
315 Hz	97,4	104,5
400 Hz	99,4	106,5
500 Hz	100,7	107,8
630 Hz	102,5	109,6
800 Hz	107,1	116,1
1000 Hz	109,8	118,8

1250 Hz	112,0	120,9
1600 Hz	107,2	109,5
2000 Hz	106,8	109,1
2500 Hz	107,3	109,6
3150 Hz	99,3	102,0
4000 Hz	91,4	94,1
5000 Hz	86,9	89,6
6300 Hz	79,7	83,6
8000 Hz	75,1	79,0
10000 Hz	70,8	74,7

,

(21)   Appendix I is amended as follows:

(a)   the title of the appendix is replaced by the following:

'**Appendix I: Database for aircraft source – Aircraft Noise and Performance (ANP) data'**

(b)   in Table I-1, the rows starting with the row "

F10062	A	D-42	0	0	0.4731	0.1565

"

up to the last row of the table are replaced by the following:

'

737800	A	A_00				0.0596977
737800	A	A_01				0.066122
737800	A	A_05				0.078996
737800	A	A_15				0.111985
737800	A	A_30			0.383611	0.117166
7378MAX	A	A_00	0	0	0	0.076682
7378MAX	A	A_00				0.056009
7378MAX	A	A_01	0	0	0	0.091438

7378MAX	A	A_01				0.066859
7378MAX	A	A_05	0	0	0	0.106627
7378MAX	A	A_05				0.077189
7378MAX	A	A_15	0	0	0.395117	0.165812
7378MAX	A	A_15				0.106525
7378MAX	A	A_30			0.375612	0.116638
7378MAX	A	A_40	0	0	0.375646	0.189672
7378MAX	D	D_00	0	0	0	0.074217
7378MAX	D	D_00				0.05418
7378MAX	D	D_01	0	0	0	0.085464
7378MAX	D	D_01				0.062526
7378MAX	D	D_05	0.00823	0.41332	0	0.101356
7378MAX	D	D_05	0.0079701	0.40898		0.074014
A350-941	A	A_1_U	0	0	0	0.05873
A350-941	A	A_1_U				0.056319
A350-941	A	A_2_D	0	0	0	0.083834
A350-941	A	A_2_D				0.081415
A350-941	A	A_2_U	0	0	0	0.06183
A350-941	A	A_2_U				0.059857
A350-941	A	A_3_D	0	0	0.219605	0.092731
A350-941	A	A_3_D			0.225785	0.092557
A350-941	A	A_FULL_D	0	0	0.214867	0.106381
A350-941	A	A_FULL_D			0.214862	0.106058
A350-941	A	A_ZERO	0	0	0	0.049173
A350-941	A	A_ZERO				0.048841
A350-941	D	D_1	0	0	0	0.052403
A350-941	D	D_1_U				0.058754
A350-941	D	D_1+F	0.00325	0.234635	0	0.06129
A350-941	D	D_1+F_D	0.002722	0.233179		0.098533
A350-941	D	D_1+F_U				0.062824
A350-941	D	D_ZERO	0	0	0	0.048142
A350-941	D	D_ZERO				0.048126

ATR72	A	15-A-G				0.0803
ATR72	A	33-A-G			0.55608	0.105
ATR72	A	ZERO-A				0.09027
ATR72	D	15	0.013155	0.538		0.08142
ATR72	D	INTR				0.07826
ATR72	D	ZERO				0.0708
F10062	A	D-42	0	0	0.4731	0.1565
F10062	A	INT2				0.0904
F10062	A	TO				0.0683
F10062	A	U-INT				0.1124
F10062	D	INT2				0.0904
F10062	D	TO	0.0122	0.5162		0.0683
F10062	D	ZERO				0.0683
F10065	A	D-42			0.4731	0.1565
F10065	A	INT2				0.0911
F10065	A	TO				0.0693
F10065	A	U-INT				0.1129
F10065	D	INT2				0.0911
F10065	D	TO	0.0123	0.521		0.0693
F10065	D	ZERO				0.0693
F28MK2	A	D-42			0.5334	0.1677
F28MK2	A	INT2				0.1033
F28MK2	A	U-INTR				0.1248
F28MK2	A	ZERO				0.0819
F28MK2	D	6	0.0171	0.6027		0.0793
F28MK2	D	INT2				0.1033
F28MK2	D	ZERO				0.0819
F28MK4	A	D-42			0.5149	0.1619
F28MK4	A	INT2				0.0971
F28MK4	A	U-INTR				0.1187
F28MK4	A	ZERO				0.0755
F28MK4	D	6	0.01515	0.5731		0.0749

F28MK4	D	INT2				0.0971
F28MK4	D	ZERO				0.0755
FAL20	A	D-25			0.804634	0.117238
FAL20	A	D-40			0.792624	0.136348
FAL20	A	INTR				0.084391
FAL20	A	ZERO				0.07
FAL20	D	10	0.035696	0.807797		0.098781
FAL20	D	INTR				0.084391
FAL20	D	ZERO				0.07
GII	A	L-0-U				0.0751
GII	A	L-10-U				0.0852
GII	A	L-20-D				0.1138
GII	A	L-39-D			0.5822	0.1742
GII	D	T-0-U				0.0814
GII	D	T-10-U				0.0884
GII	D	T-20-D	0.02	0.634		0.1159
GIIB	A	L-0-U				0.0722
GIIB	A	L-10-U				0.0735
GIIB	A	L-20-D				0.1091
GIIB	A	L-39-D			0.562984	0.1509
GIIB	D	T-0-U				0.0738
GIIB	D	T-10-U				0.0729
GIIB	D	T-20-D	0.0162	0.583		0.1063
GIV	A	L-0-U				0.06
GIV	A	L-20-D				0.1063
GIV	A	L-39-D			0.5805	0.1403
GIV	D	T-0-U				0.0586
GIV	D	T-10-U				0.0666
GIV	D	T-20-D	0.0146	0.5798		0.1035
GIV	D	T-20-U				0.0797
GV	A	L-0-U				0.0617
GV	A	L-20-D				0.0974

GV	A	L-20-U				0.0749
GV	A	L-39-D			0.4908	0.1328
GV	D	T-0-U				0.058
GV	D	T-10-U				0.0606
GV	D	T-20-D	0.01178	0.516		0.0953
GV	D	T-20-U				0.0743
HS748A	A	D-30			0.45813	0.13849
HS748A	A	D-INTR				0.106745
HS748A	A	INTR				0.088176
HS748A	A	ZERO				0.075
HS748A	D	INTR				0.088176
HS748A	D	TO	0.012271	0.542574		0.101351
HS748A	D	ZERO				0.075
IA1125	A	D-40			0.967478	0.136393
IA1125	A	D-INTR				0.118618
IA1125	A	INTR				0.085422
IA1125	A	ZERO				0.07
IA1125	D	12	0.040745	0.963488		0.100843
IA1125	D	INTR				0.085422
IA1125	D	ZERO				0.07
L1011	A	10				0.093396
L1011	A	D-33			0.286984	0.137671
L1011	A	D-42			0.256389	0.155717
L1011	A	ZERO				0.06243
L1011	D	10	0.004561	0.265314		0.093396
L1011	D	22	0.004759	0.251916		0.105083
L1011	D	INTR				0.07959
L1011	D	ZERO				0.06243
L10115	A	10				0.093396
L10115	A	D-33			0.262728	0.140162
L10115	A	D-42			0.256123	0.155644
L10115	A	ZERO				0.06243

L10115	D	10	0.004499	0.265314		0.093396
L10115	D	22	0.004695	0.251916		0.105083
L10115	D	INTR				0.07959
L10115	D	ZERO				0.06243
L188	A	D-100			0.436792	0.174786
L188	A	D-78-%			0.456156	0.122326
L188	A	INTR				0.120987
L188	A	ZERO				0.082
L188	D	39-%	0.009995	0.420533		0.142992
L188	D	78-%	0.010265	0.404302		0.159974
L188	D	INTR				0.120987
L188	D	ZERO				0.082
LEAR25	A	10				0.09667
LEAR25	A	D-40			1.28239	0.176632
LEAR25	A	D-INTR				0.149986
LEAR25	A	ZERO				0.07
LEAR25	D	10				0.09667
LEAR25	D	20	0.082866	1.27373		0.12334
LEAR25	D	ZERO				0.07
LEAR35	A	10				0.089112
LEAR35	A	D-40			1.08756	0.150688
LEAR35	A	D-INTR				0.129456
LEAR35	A	ZERO				0.07
LEAR35	D	10				0.089112
LEAR35	D	20	0.043803	1.05985		0.108224
LEAR35	D	ZERO				0.07
MD11GE	D	10	0.003812	0.2648		0.0843
MD11GE	D	15	0.003625	0.2578		0.0891
MD11GE	D	20	0.003509	0.2524		0.0947
MD11GE	D	25	0.003443	0.2481		0.1016
MD11GE	D	0/EXT				0.0692
MD11GE	D	0/RET				0.0551

MD11GE	D	ZERO				0.0551
MD11PW	D	10	0.003829	0.265		0.08425
MD11PW	D	15	0.003675	0.2576		0.08877
MD11PW	D	20	0.003545	0.2526		0.09472
MD11PW	D	25	0.003494	0.2487		0.1018
MD11PW	D	0/EXT				0.0691
MD11PW	D	0/RET				0.05512
MD11PW	D	ZERO				0.05512
MD81	D	11	0.009276	0.4247		0.07719
MD81	D	INT1				0.07643
MD81	D	INT2				0.06313
MD81	D	INT3				0.06156
MD81	D	INT4				0.06366
MD81	D	T_15	0.009369	0.420798		0.0857
MD81	D	T_INT				0.0701
MD81	D	T_ZERO				0.061
MD81	D	ZERO				0.06761
MD82	D	11	0.009248	0.4236		0.07969
MD82	D	INT1				0.07625
MD82	D	INT2				0.06337
MD82	D	INT3				0.06196
MD82	D	INT4				0.0634
MD82	D	T_15	0.009267	0.420216		0.086
MD82	D	T_INT				0.065
MD82	D	T_ZERO				0.061
MD82	D	ZERO				0.06643
MD83	D	11	0.009301	0.4227		0.0798
MD83	D	INT1				0.07666
MD83	D	INT2				0.0664
MD83	D	INT3				0.06247
MD83	D	INT4				0.06236
MD83	D	T_15	0.009384	0.420307		0.086

MD83	D	T_INT				0.0664
MD83	D	T_ZERO				0.0611
MD83	D	ZERO				0.06573
MD9025	A	D-28			0.4118	0.1181
MD9025	A	D-40			0.4003	0.1412
MD9025	A	U-0			0.4744	0.0876
MD9025	D	EXT/06	0.010708	0.458611		0.070601
MD9025	D	EXT/11	0.009927	0.441118		0.073655
MD9025	D	EXT/18	0.009203	0.421346		0.083277
MD9025	D	EXT/24	0.008712	0.408301		0.090279
MD9025	D	RET/0				0.05186
MD9028	A	D-28			0.4118	0.1181
MD9028	A	D-40			0.4003	0.1412
MD9028	A	U-0			0.4744	0.0876
MD9028	D	EXT/06	0.010993	0.463088		0.070248
MD9028	D	EXT/11	0.010269	0.446501		0.072708
MD9028	D	EXT/18	0.009514	0.426673		0.082666
MD9028	D	EXT/24	0.008991	0.413409		0.090018
MD9028	D	RET/0				0.05025
MU3001	A	1				0.08188
MU3001	A	D-30			1.07308	0.147487
MU3001	A	D-INTR				0.114684
MU3001	A	ZERO				0.07
MU3001	D	1	0.065703	1.1529		0.08188
MU3001	D	10	0.055318	1.0729		0.09285
MU3001	D	ZERO				0.07
PA30	A	27-A			1.316667	0.104586
PA30	A	ZERO-A				0.078131
PA30	D	15-D	0.100146	1.166667		0.154071
PA30	D	ZERO-D				0.067504
PA42	A	30-DN			1.09213	0.14679
PA42	A	ZERO-A				0.087856

PA42	D	ZER-DN	0.06796	1.011055		0.08088
PA42	D	ZERO				0.087856
PA42	D	ZERO-C				0.139096
PA42	D	ZERO-T				0.07651
SD330	A	D-15			0.746802	0.109263
SD330	A	D-35			0.702872	0.143475
SD330	A	INTR				0.106596
SD330	A	ZERO				0.075
SD330	D	10	0.031762	0.727556		0.138193
SD330	D	INTR				0.106596
SD330	D	ZERO				0.075
SF340	A	5				0.105831
SF340	A	D-35			0.75674	0.147912
SF340	A	D-INTR				0.111456
SF340	A	ZERO				0.075
SF340	D	5				0.105831
SF340	D	15	0.026303	0.746174		0.136662
SF340	D	ZERO				0.075

'

(c)   in Table I-2, the rows corresponding to the AIRCFTID 737700 and 737800 are correspondingly replaced by:

'

737700	Boeing 737-700/CFM56-7B24	Jet	2	Large	Commercial	154500	129200	4445	24000	3	CF567B	CNT (lb)	206	104	Wing
737800	Boeing 737-800 / CFM56-7B26	Jet	2	Large	Commercial	174200	146300	5435	26300	3	CF567B	CNT (lb)	206	104	Wing

'

(d)   in Table I-2, the following rows are added:

'

7378MAX	Boeing 737 MAX 8 / CFM Leap1B-27	Jet	2	Large	Commercial	181200	152800	4965	26400	4	7378MAX	CNT (lb)	216	103	Wing
A350-941	Airbus A350-941 / RR Trent XWB-84	Jet	2	Heavy	Commercial	610681	456356	6558	84200	4	A350-941	CNT (lb)	239	139	Wing
ATR72	Avions de Transport Regional ATR 72-212A / PW127F	Turboprop	2	Large	Commercial	50710	49270	3360	7587	4	ATR72	CNT (lb)	240	140	Prop

,

(e)   In Table I-3, the following rows are added:

'

737800	DEFAULT	1	Descend-Idle	A_00	6000	248.93	3			
737800	DEFAULT	2	Level-Idle	A_00	3000	249.5			25437	
737800	DEFAULT	3	Level-Idle	A_01	3000	187.18			3671	
737800	DEFAULT	4	Level-Idle	A_05	3000	174.66			5209	
737800	DEFAULT	5	Descend-Idle	A_15	3000	151.41	3			
737800	DEFAULT	6	Descend	A_30	2817	139.11	3			
737800	DEFAULT	7	Land	A_30				393.8		
737800	DEFAULT	8	Decelerate	A_30		139			3837.5	40
737800	DEFAULT	9	Decelerate	A_30		30			0	10
737MAX8	DEFAULT	1	Descend-Idle	A_00	6000	249.2	3			
737MAX8	DEFAULT	2	Level-Idle	A_00	3000	249.7			24557	
737MAX8	DEFAULT	3	Level-Idle	A_01	3000	188.5			4678	
737MAX8	DEFAULT	4	Level-Idle	A_05	3000	173.7			4907	

737MAX8	DEFAULT	5	Descend-Idle	A_15	3000	152	3			
737MAX8	DEFAULT	6	Descend	A_30	2817	139	3			
737MAX8	DEFAULT	7	Land	A_30				393.8		
737MAX8	DEFAULT	8	Decelerate	A_30		139			3837.5	40
737MAX8	DEFAULT	9	Decelerate	A_30		30			0	10
A350-941	DEFAULT 1	1	Descend-Idle	A_ZERO	6000	250	2.74			
A350-941	DEFAULT 1	2	Level-Idle	A_ZERO	3000	250			26122	
A350-941	DEFAULT 1	3	Level-Idle	A_1_U	3000	188.6			6397.6	
A350-941	DEFAULT 1	4	Descend-Idle	A_1_U	3000	168.4	3			
A350-941	DEFAULT 1	5	Descend-Idle	A_2_D	2709	161.9	3			
A350-941	DEFAULT 1	6	Descend-Idle	A_3_D	2494	155.2	3			
A350-941	DEFAULT 1	7	Descend	A_FULL_D	2180	137.5	3			
A350-941	DEFAULT 1	8	Descend	A_FULL_D	50	137.5	3			
A350-941	DEFAULT 1	9	Land	A_FULL_D				556.1		
A350-941	DEFAULT 1	10	Decelerate	A_FULL_D		137.5			5004.9	10
A350-941	DEFAULT 1	11	Decelerate	A_FULL_D		30			0	10
A350-941	DEFAULT 2	1	Descend-Idle	A_ZERO	6000	250	2.74			
A350-941	DEFAULT 2	2	Level-Idle	A_ZERO	3000	250			26122	
A350-941	DEFAULT 2	3	Level	A_1_U	3000	188.6			20219.8	
A350-941	DEFAULT 2	4	Level-Idle	A_1_U	3000	188.6			6049.9	
A350-941	DEFAULT 2	5	Descend-Idle	A_1_U	3000	168.3	3			
A350-941	DEFAULT 2	6	Descend-Idle	A_2_D	2709	161.8	3			
A350-941	DEFAULT 2	7	Descend	A_FULL_D	2180	137.5	3			
A350-941	DEFAULT	8	Descend	A_FULL_	50	137.5	3			

	2			D							
A350-941	DEFAULT 2	9	Land	A_FULL_D				556.1			
A350-941	DEFAULT 2	10	Decelerate	A_FULL_D		137.5				5004.9	10
A350-941	DEFAULT 2	11	Decelerate	A_FULL_D		30				0	10
ATR72	DEFAULT	1	Descend	ZERO-A	6000	238	3				
ATR72	DEFAULT	2	Level-Decel	ZERO-A	3000	238			17085		
ATR72	DEFAULT	3	Level-Decel	15-A-G	3000	158.3			3236		
ATR72	DEFAULT	4	Level	15-A-G	3000	139			3521		
ATR72	DEFAULT	5	Level	33-A-G	3000	139			3522		
ATR72	DEFAULT	6	Descend-Decel	33-A-G	3000	139	3				
ATR72	DEFAULT	7	Descend	33-A-G	2802	117.1	3				
ATR72	DEFAULT	8	Descend	33-A-G	50	117.1	3				
ATR72	DEFAULT	9	Land	33-A-G				50			
ATR72	DEFAULT	10	Decelerate	33-A-G		114.2			1218	75.9	
ATR72	DEFAULT	11	Decelerate	33-A-G		30			0	5.7	

'

(f)   in Table I-4 (part 1), the following rows are added:

'

737MAX8	DEFAULT	1	1	Takeoff	MaxTakeoff	D_05				
737MAX8	DEFAULT	1	2	Climb	MaxTakeoff	D_05	1000			
737MAX8	DEFAULT	1	3	Accelerate	MaxClimb	D_05		1336	174	
737MAX8	DEFAULT	1	4	Accelerate	MaxClimb	D_01		1799	205	
737MAX8	DEFAULT	1	5	Climb	MaxClimb	D_00	3000			
737MAX8	DEFAULT	1	6	Accelerate	MaxClimb	D_00		1681	250	
737MAX8	DEFAULT	1	7	Climb	MaxClimb	D_00	5500			
737MAX8	DEFAULT	1	8	Climb	MaxClimb	D_00	7500			
737MAX8	DEFAULT	1	9	Climb	MaxClimb	D_00	10000			
737MAX8	DEFAULT	2	1	Takeoff	MaxTakeoff	D_05				
737MAX8	DEFAULT	2	2	Climb	MaxTakeoff	D_05	1000			

737MAX8	DEFAULT	2	3	Accelerate	MaxClimb	D_05		1284	176	
737MAX8	DEFAULT	2	4	Accelerate	MaxClimb	D_01		1651	208	
737MAX8	DEFAULT	2	5	Climb	MaxClimb	D_00	3000			
737MAX8	DEFAULT	2	6	Accelerate	MaxClimb	D_00		1619	250	
737MAX8	DEFAULT	2	7	Climb	MaxClimb	D_00	5500			
737MAX8	DEFAULT	2	8	Climb	MaxClimb	D_00	7500			
737MAX8	DEFAULT	2	9	Climb	MaxClimb	D_00	10000			
737MAX8	DEFAULT	3	1	Takeoff	MaxTakeoff	D_05				
737MAX8	DEFAULT	3	2	Climb	MaxTakeoff	D_05	1000			
737MAX8	DEFAULT	3	3	Accelerate	MaxClimb	D_05		1229	177	
737MAX8	DEFAULT	3	4	Accelerate	MaxClimb	D_01		1510	210	
737MAX8	DEFAULT	3	5	Climb	MaxClimb	D_00	3000			
737MAX8	DEFAULT	3	6	Accelerate	MaxClimb	D_00		1544	250	
737MAX8	DEFAULT	3	7	Climb	MaxClimb	D_00	5500			
737MAX8	DEFAULT	3	8	Climb	MaxClimb	D_00	7500			
737MAX8	DEFAULT	3	9	Climb	MaxClimb	D_00	10000			
737MAX8	DEFAULT	4	1	Takeoff	MaxTakeoff	D_05				
737MAX8	DEFAULT	4	2	Climb	MaxTakeoff	D_05	1000			
737MAX8	DEFAULT	4	3	Accelerate	MaxClimb	D_05		1144	181	
737MAX8	DEFAULT	4	4	Accelerate	MaxClimb	D_01		1268	213	
737MAX8	DEFAULT	4	5	Climb	MaxClimb	D_00	3000			
737MAX8	DEFAULT	4	6	Accelerate	MaxClimb	D_00		1414	250	
737MAX8	DEFAULT	4	7	Climb	MaxClimb	D_00	5500			
737MAX8	DEFAULT	4	8	Climb	MaxClimb	D_00	7500			
737MAX8	DEFAULT	4	9	Climb	MaxClimb	D_00	10000			
737MAX8	DEFAULT	5	1	Takeoff	MaxTakeoff	D_05				
737MAX8	DEFAULT	5	2	Climb	MaxTakeoff	D_05	1000			
737MAX8	DEFAULT	5	3	Accelerate	MaxClimb	D_05		1032	184	
737MAX8	DEFAULT	5	4	Accelerate	MaxClimb	D_01		1150	217	
737MAX8	DEFAULT	5	5	Climb	MaxClimb	D_00	3000			
737MAX8	DEFAULT	5	6	Accelerate	MaxClimb	D_00		1292	250	
737MAX8	DEFAULT	5	7	Climb	MaxClimb	D_00	5500			

737MAX8	DEFAULT	5	8	Climb	MaxClimb	D_00	7500			
737MAX8	DEFAULT	5	9	Climb	MaxClimb	D_00	10000			
737MAX8	DEFAULT	6	1	Takeoff	MaxTakeoff	D_05				
737MAX8	DEFAULT	6	2	Climb	MaxTakeoff	D_05	1000			
737MAX8	DEFAULT	6	3	Accelerate	MaxClimb	D_05		1001	185	
737MAX8	DEFAULT	6	4	Accelerate	MaxClimb	D_01		1120	219	
737MAX8	DEFAULT	6	5	Climb	MaxClimb	D_00	3000			
737MAX8	DEFAULT	6	6	Accelerate	MaxClimb	D_00		1263	250	
737MAX8	DEFAULT	6	7	Climb	MaxClimb	D_00	5500			
737MAX8	DEFAULT	6	8	Climb	MaxClimb	D_00	7500			
737MAX8	DEFAULT	6	9	Climb	MaxClimb	D_00	10000			
737MAX8	DEFAULT	M	1	Takeoff	MaxTakeoff	D_05				
737MAX8	DEFAULT	M	2	Climb	MaxTakeoff	D_05	1000			
737MAX8	DEFAULT	M	3	Accelerate	MaxClimb	D_05		951	188	
737MAX8	DEFAULT	M	4	Accelerate	MaxClimb	D_01		1058	221	
737MAX8	DEFAULT	M	5	Climb	MaxClimb	D_00	3000			
737MAX8	DEFAULT	M	6	Accelerate	MaxClimb	D_00		1196	250	
737MAX8	DEFAULT	M	7	Climb	MaxClimb	D_00	5500			
737MAX8	DEFAULT	M	8	Climb	MaxClimb	D_00	7500			
737MAX8	DEFAULT	M	9	Climb	MaxClimb	D_00	10000			
737MAX8	ICAO_A	1	1	Takeoff	MaxTakeoff	D_05				
737MAX8	ICAO_A	1	2	Climb	MaxTakeoff	D_05	1500			
737MAX8	ICAO_A	1	3	Climb	MaxClimb	D_05	3000			
737MAX8	ICAO_A	1	4	Accelerate	MaxClimb	D_05		1300	174	
737MAX8	ICAO_A	1	5	Accelerate	MaxClimb	D_01		1667	205	
737MAX8	ICAO_A	1	6	Accelerate	MaxClimb	D_00		2370	250	
737MAX8	ICAO_A	1	7	Climb	MaxClimb	D_00	5500			
737MAX8	ICAO_A	1	8	Climb	MaxClimb	D_00	7500			
737MAX8	ICAO_A	1	9	Climb	MaxClimb	D_00	10000			
737MAX8	ICAO_A	2	1	Takeoff	MaxTakeoff	D_05				
737MAX8	ICAO_A	2	2	Climb	MaxTakeoff	D_05	1500			
737MAX8	ICAO_A	2	3	Climb	MaxClimb	D_05	3000			

737MAX8	ICAO_A	2	4	Accelerate	MaxClimb	D_05		1243	174	
737MAX8	ICAO_A	2	5	Accelerate	MaxClimb	D_01		1524	207	
737MAX8	ICAO_A	2	6	Accelerate	MaxClimb	D_00		2190	250	
737MAX8	ICAO_A	2	7	Climb	MaxClimb	D_00	5500			
737MAX8	ICAO_A	2	8	Climb	MaxClimb	D_00	7500			
737MAX8	ICAO_A	2	9	Climb	MaxClimb	D_00	10000			
737MAX8	ICAO_A	3	1	Takeoff	MaxTakeoff	D_05				
737MAX8	ICAO_A	3	2	Climb	MaxTakeoff	D_05	1500			
737MAX8	ICAO_A	3	3	Climb	MaxClimb	D_05	3000			
737MAX8	ICAO_A	3	4	Accelerate	MaxClimb	D_05		1190	176	
737MAX8	ICAO_A	3	5	Accelerate	MaxClimb	D_01		1331	210	
737MAX8	ICAO_A	3	6	Accelerate	MaxClimb	D_00		2131	250	
737MAX8	ICAO_A	3	7	Climb	MaxClimb	D_00	5500			
737MAX8	ICAO_A	3	8	Climb	MaxClimb	D_00	7500			
737MAX8	ICAO_A	3	9	Climb	MaxClimb	D_00	10000			
737MAX8	ICAO_A	4	1	Takeoff	MaxTakeoff	D_05				
737MAX8	ICAO_A	4	2	Climb	MaxTakeoff	D_05	1500			
737MAX8	ICAO_A	4	3	Climb	MaxClimb	D_05	3000			
737MAX8	ICAO_A	4	4	Accelerate	MaxClimb	D_05		1098	180	
737MAX8	ICAO_A	4	5	Accelerate	MaxClimb	D_01		1221	211	
737MAX8	ICAO_A	4	6	Accelerate	MaxClimb	D_00		1883	250	
737MAX8	ICAO_A	4	7	Climb	MaxClimb	D_00	5500			
737MAX8	ICAO_A	4	8	Climb	MaxClimb	D_00	7500			
737MAX8	ICAO_A	4	9	Climb	MaxClimb	D_00	10000			
737MAX8	ICAO_A	5	1	Takeoff	MaxTakeoff	D_05				
737MAX8	ICAO_A	5	2	Climb	MaxTakeoff	D_05	1500			
737MAX8	ICAO_A	5	3	Climb	MaxClimb	D_05	3000			
737MAX8	ICAO_A	5	4	Accelerate	MaxClimb	D_05		988	183	
737MAX8	ICAO_A	5	5	Accelerate	MaxClimb	D_01		1101	216	
737MAX8	ICAO_A	5	6	Accelerate	MaxClimb	D_00		1730	250	
737MAX8	ICAO_A	5	7	Climb	MaxClimb	D_00	5500			
737MAX8	ICAO_A	5	8	Climb	MaxClimb	D_00	7500			

737MAX8	ICAO_A	5	9	Climb	MaxClimb	D_00	10000		
737MAX8	ICAO_A	6	1	Takeoff	MaxTakeoff	D_05			
737MAX8	ICAO_A	6	2	Climb	MaxTakeoff	D_05	1500		
737MAX8	ICAO_A	6	3	Climb	MaxClimb	D_05	3000		
737MAX8	ICAO_A	6	4	Accelerate	MaxClimb	D_05		964	185
737MAX8	ICAO_A	6	5	Accelerate	MaxClimb	D_01		1073	217
737MAX8	ICAO_A	6	6	Accelerate	MaxClimb	D_00		1588	250
737MAX8	ICAO_A	6	7	Climb	MaxClimb	D_00	5500		
737MAX8	ICAO_A	6	8	Climb	MaxClimb	D_00	7500		
737MAX8	ICAO_A	6	9	Climb	MaxClimb	D_00	10000		
737MAX8	ICAO_A	M	1	Takeoff	MaxTakeoff	D_05			
737MAX8	ICAO_A	M	2	Climb	MaxTakeoff	D_05	1500		
737MAX8	ICAO_A	M	3	Climb	MaxClimb	D_05	3000		
737MAX8	ICAO_A	M	4	Accelerate	MaxClimb	D_05		911	187
737MAX8	ICAO_A	M	5	Accelerate	MaxClimb	D_01		1012	220
737MAX8	ICAO_A	M	6	Accelerate	MaxClimb	D_00		1163	250
737MAX8	ICAO_A	M	7	Climb	MaxClimb	D_00	5500		
737MAX8	ICAO_A	M	8	Climb	MaxClimb	D_00	7500		
737MAX8	ICAO_A	M	9	Climb	MaxClimb	D_00	10000		
737MAX8	ICAO_B	1	1	Takeoff	MaxTakeoff	D_05			
737MAX8	ICAO_B	1	2	Climb	MaxTakeoff	D_05	1000		
737MAX8	ICAO_B	1	3	Accelerate	MaxTakeoff	D_01		1734	178
737MAX8	ICAO_B	1	4	Accelerate	MaxTakeoff	D_00		2595	205
737MAX8	ICAO_B	1	5	Climb	MaxClimb	D_00	3000		
737MAX8	ICAO_B	1	6	Accelerate	MaxClimb	D_00		1671	250
737MAX8	ICAO_B	1	7	Climb	MaxClimb	D_00	5500		
737MAX8	ICAO_B	1	8	Climb	MaxClimb	D_00	7500		
737MAX8	ICAO_B	1	9	Climb	MaxClimb	D_00	10000		
737MAX8	ICAO_B	2	1	Takeoff	MaxTakeoff	D_05			
737MAX8	ICAO_B	2	2	Climb	MaxTakeoff	D_05	1000		
737MAX8	ICAO_B	2	3	Accelerate	MaxTakeoff	D_01		1682	179
737MAX8	ICAO_B	2	4	Accelerate	MaxTakeoff	D_00		2477	208

737MAX8	ICAO_B	2	5	Climb	MaxClimb	D_00	3000			
737MAX8	ICAO_B	2	6	Accelerate	MaxClimb	D_00		1610	250	
737MAX8	ICAO_B	2	7	Climb	MaxClimb	D_00	5500			
737MAX8	ICAO_B	2	8	Climb	MaxClimb	D_00	7500			
737MAX8	ICAO_B	2	9	Climb	MaxClimb	D_00	10000			
737MAX8	ICAO_B	3	1	Takeoff	MaxTakeoff	D_05				
737MAX8	ICAO_B	3	2	Climb	MaxTakeoff	D_05	1000			
737MAX8	ICAO_B	3	3	Accelerate	MaxTakeoff	D_01		1616	180	
737MAX8	ICAO_B	3	4	Accelerate	MaxTakeoff	D_00		2280	210	
737MAX8	ICAO_B	3	5	Climb	MaxClimb	D_00	3000			
737MAX8	ICAO_B	3	6	Accelerate	MaxClimb	D_00		1545	250	
737MAX8	ICAO_B	3	7	Climb	MaxClimb	D_00	5500			
737MAX8	ICAO_B	3	8	Climb	MaxClimb	D_00	7500			
737MAX8	ICAO_B	3	9	Climb	MaxClimb	D_00	10000			
737MAX8	ICAO_B	4	1	Takeoff	MaxTakeoff	D_05				
737MAX8	ICAO_B	4	2	Climb	MaxTakeoff	D_05	1000			
737MAX8	ICAO_B	4	3	Accelerate	MaxTakeoff	D_01		1509	184	
737MAX8	ICAO_B	4	4	Accelerate	MaxTakeoff	D_00		2103	214	
737MAX8	ICAO_B	4	5	Climb	MaxClimb	D_00	3000			
737MAX8	ICAO_B	4	6	Accelerate	MaxClimb	D_00		1589	250	
737MAX8	ICAO_B	4	7	Climb	MaxClimb	D_00	5500			
737MAX8	ICAO_B	4	8	Climb	MaxClimb	D_00	7500			
737MAX8	ICAO_B	4	9	Climb	MaxClimb	D_00	10000			
737MAX8	ICAO_B	5	1	Takeoff	MaxTakeoff	D_05				
737MAX8	ICAO_B	5	2	Climb	MaxTakeoff	D_05	1000			
737MAX8	ICAO_B	5	3	Accelerate	MaxTakeoff	D_01		1388	188	
737MAX8	ICAO_B	5	4	Accelerate	MaxTakeoff	D_00		1753	220	
737MAX8	ICAO_B	5	5	Climb	MaxClimb	D_00	3000			
737MAX8	ICAO_B	5	6	Accelerate	MaxClimb	D_00		1295	250	
737MAX8	ICAO_B	5	7	Climb	MaxClimb	D_00	5500			
737MAX8	ICAO_B	5	8	Climb	MaxClimb	D_00	7500			
737MAX8	ICAO_B	5	9	Climb	MaxClimb	D_00	10000			

737MAX8	ICAO_B	6	1	Takeoff	MaxTakeoff	D_05				
737MAX8	ICAO_B	6	2	Climb	MaxTakeoff	D_05	1000			
737MAX8	ICAO_B	6	3	Accelerate	MaxTakeoff	D_01		1345	188	
737MAX8	ICAO_B	6	4	Accelerate	MaxTakeoff	D_00		1634	220	
737MAX8	ICAO_B	6	5	Climb	MaxClimb	D_00	3000			
737MAX8	ICAO_B	6	6	Accelerate	MaxClimb	D_00		1262	250	
737MAX8	ICAO_B	6	7	Climb	MaxClimb	D_00	5500			
737MAX8	ICAO_B	6	8	Climb	MaxClimb	D_00	7500			
737MAX8	ICAO_B	6	9	Climb	MaxClimb	D_00	10000			
737MAX8	ICAO_B	M	1	Takeoff	MaxTakeoff	D_05				
737MAX8	ICAO_B	M	2	Climb	MaxTakeoff	D_05	1000			
737MAX8	ICAO_B	M	3	Accelerate	MaxTakeoff	D_01		1287	191	
737MAX8	ICAO_B	M	4	Accelerate	MaxTakeoff	D_00		1426	225	
737MAX8	ICAO_B	M	5	Climb	MaxClimb	D_00	3000			
737MAX8	ICAO_B	M	6	Accelerate	MaxClimb	D_00		1196	250	
737MAX8	ICAO_B	M	7	Climb	MaxClimb	D_00	5500			
737MAX8	ICAO_B	M	8	Climb	MaxClimb	D_00	7500			
737MAX8	ICAO_B	M	9	Climb	MaxClimb	D_00	10000			

'

(g)   in Table I-4 (part 2), the following rows are added:

'

A350-941	DEFAULT	1	1	Takeoff	MaxTakeoff	D_1+F_D				
A350-941	DEFAULT	1	2	Climb	MaxTakeoff	D_1+F_D	1000			
A350-941	DEFAULT	1	3	Accelerate	MaxTakeoff	D_1+F_U		1726.5	170.7	60
A350-941	DEFAULT	1	4	Accelerate	MaxTakeoff	D_1_U		1862.6	197.2	60
A350-941	DEFAULT	1	5	Climb	MaxClimb	D_ZERO	3000			
A350-941	DEFAULT	1	6	Accelerate	MaxClimb	D_ZERO		1658	250	60
A350-941	DEFAULT	1	7	Climb	MaxClimb	D_ZERO	10000			
A350-941	DEFAULT	2	1	Takeoff	MaxTakeoff	D_1+F_D				
A350-941	DEFAULT	2	2	Climb	MaxTakeoff	D_1+F_D	1000			

A350-941	DEFAULT	2	3	Accelerate	MaxTakeoff	D_1+F_U		1699.9	173.1	60
A350-941	DEFAULT	2	4	Accelerate	MaxTakeoff	D_1_U		1812.6	198.6	60
A350-941	DEFAULT	2	5	Climb	MaxClimb	D_ZERO	3000			
A350-941	DEFAULT	2	6	Accelerate	MaxClimb	D_ZERO		1604.5	250	60
A350-941	DEFAULT	2	7	Climb	MaxClimb	D_ZERO	10000			
A350-941	DEFAULT	3	1	Takeoff	MaxTakeoff	D_1+F_D				
A350-941	DEFAULT	3	2	Climb	MaxTakeoff	D_1+F_D	1000			
A350-941	DEFAULT	3	3	Accelerate	MaxTakeoff	D_1+F_U		1662.2	175.6	60
A350-941	DEFAULT	3	4	Accelerate	MaxTakeoff	D_1_U		1762.3	200.1	60
A350-941	DEFAULT	3	5	Climb	MaxClimb	D_ZERO	3000			
A350-941	DEFAULT	3	6	Accelerate	MaxClimb	D_ZERO		1551.6	250	60
A350-941	DEFAULT	3	7	Climb	MaxClimb	D_ZERO	10000			
A350-941	DEFAULT	4	1	Takeoff	MaxTakeoff	D_1+F_D				
A350-941	DEFAULT	4	2	Climb	MaxTakeoff	D_1+F_U	1000			
A350-941	DEFAULT	4	3	Accelerate	MaxTakeoff	D_1+F_U		1586.1	179.9	60
A350-941	DEFAULT	4	4	Accelerate	MaxTakeoff	D_1_U		1679.8	202.7	60
A350-941	DEFAULT	4	5	Climb	MaxClimb	D_ZERO	3000			
A350-941	DEFAULT	4	6	Accelerate	MaxClimb	D_ZERO		1465.3	250	60
A350-941	DEFAULT	4	7	Climb	MaxClimb	D_ZERO	10000			
A350-941	DEFAULT	5	1	Takeoff	MaxTakeoff	D_1+F_D				
A350-941	DEFAULT	5	2	Climb	MaxTakeoff	D_1+F_U	1000			
A350-941	DEFAULT	5	3	Accelerate	MaxTakeoff	D_1+F_U		1491.7	185.3	60
A350-941	DEFAULT	5	4	Accelerate	MaxTakeoff	D_1_U		1586.9	206.4	60
A350-941	DEFAULT	5	5	Climb	MaxClimb	D_ZERO	3000			
A350-941	DEFAULT	5	6	Accelerate	MaxClimb	D_ZERO		1365.5	250	60
A350-941	DEFAULT	5	7	Climb	MaxClimb	D_ZERO	10000			
A350-941	DEFAULT	6	1	Takeoff	MaxTakeoff	D_1+F_D				
A350-941	DEFAULT	6	2	Climb	MaxTakeoff	D_1+F_U	1000			
A350-941	DEFAULT	6	3	Accelerate	MaxTakeoff	D_1+F_U		1399.5	191.1	60
A350-941	DEFAULT	6	4	Accelerate	MaxTakeoff	D_1_U		1494.1	210.4	60
A350-941	DEFAULT	6	5	Climb	MaxClimb	D_ZERO	3000			
A350-941	DEFAULT	6	6	Accelerate	MaxClimb	D_ZERO		1268.2	250	60

A350-941	DEFAULT	6	7	Climb	MaxClimb	D_ZERO	10000			
A350-941	DEFAULT	7	1	Takeoff	MaxTakeoff	D_1+F_D				
A350-941	DEFAULT	7	2	Climb	MaxTakeoff	D_1+F_U	1000			
A350-941	DEFAULT	7	3	Accelerate	MaxTakeoff	D_1+F_U		1314	197	60
A350-941	DEFAULT	7	4	Accelerate	MaxTakeoff	D_1_U		1407.1	214.7	60
A350-941	DEFAULT	7	5	Climb	MaxClimb	D_ZERO	3000			
A350-941	DEFAULT	7	6	Accelerate	MaxClimb	D_ZERO		1176.3	250	60
A350-941	DEFAULT	7	7	Climb	MaxClimb	D_ZERO	10000			
A350-941	DEFAULT	8	1	Takeoff	MaxTakeoff	D_1+F_D				
A350-941	DEFAULT	8	2	Climb	MaxTakeoff	D_1+F_U	1000			
A350-941	DEFAULT	8	3	Accelerate	MaxTakeoff	D_1+F_U		1233.3	203.4	60
A350-941	DEFAULT	8	4	Accelerate	MaxTakeoff	D_1_U		1325.3	219.6	60
A350-941	DEFAULT	8	5	Climb	MaxClimb	D_ZERO	3000			
A350-941	DEFAULT	8	6	Accelerate	MaxClimb	D_ZERO		1089.2	250	60
A350-941	DEFAULT	8	7	Climb	MaxClimb	D_ZERO	10000			
A350-941	DEFAULT	M	1	Takeoff	MaxTakeoff	D_1+F_D				
A350-941	DEFAULT	M	2	Climb	MaxTakeoff	D_1+F_U	1000			
A350-941	DEFAULT	M	3	Accelerate	MaxTakeoff	D_1+F_U		1185.1	207.6	60
A350-941	DEFAULT	M	4	Accelerate	MaxTakeoff	D_1_U		1275.6	222.9	60
A350-941	DEFAULT	M	5	Climb	MaxClimb	D_ZERO	3000			
A350-941	DEFAULT	M	6	Accelerate	MaxClimb	D_ZERO		1036.7	250	60
A350-941	DEFAULT	M	7	Climb	MaxClimb	D_ZERO	10000			
A350-941	ICAO_A	1	1	Takeoff	MaxTakeoff	D_1+F_D				
A350-941	ICAO_A	1	2	Climb	MaxTakeoff	D_1+F_U	1500			
A350-941	ICAO_A	1	3	Climb	MaxClimb	D_1+F_U	3000			
A350-941	ICAO_A	1	4	Accelerate	MaxClimb	D_1+F_U		1323.2	171	60
A350-941	ICAO_A	1	5	Accelerate	MaxClimb	D_1_U		1353.1	189.5	60
A350-941	ICAO_A	1	6	Accelerate	MaxClimb	D_ZERO		1514.1	213.7	60
A350-941	ICAO_A	1	7	Accelerate	MaxClimb	D_ZERO		1673.8	250	60
A350-941	ICAO_A	1	8	Climb	MaxClimb	D_ZERO	10000			
A350-941	ICAO_A	2	1	Takeoff	MaxTakeoff	D_1+F_D				
A350-941	ICAO_A	2	2	Climb	MaxTakeoff	D_1+F_U	1500			

A350-941	ICAO_A	2	3	Climb	MaxClimb	D_1+F_U	3000			
A350-941	ICAO_A	2	4	Accelerate	MaxClimb	D_1+F_U		1265.7	173.4	60
A350-941	ICAO_A	2	5	Accelerate	MaxClimb	D_1_U		1315.1	191.2	60
A350-941	ICAO_A	2	6	Accelerate	MaxClimb	D_ZERO		1466.2	214.5	60
A350-941	ICAO_A	2	7	Accelerate	MaxClimb	D_ZERO		1619.3	250	60
A350-941	ICAO_A	2	8	Climb	MaxClimb	D_ZERO	10000			
A350-941	ICAO_A	3	1	Takeoff	MaxTakeoff	D_1+F_D				
A350-941	ICAO_A	3	2	Climb	MaxTakeoff	D_1+F_U	1500			
A350-941	ICAO_A	3	3	Climb	MaxClimb	D_1+F_U	3000			
A350-941	ICAO_A	3	4	Accelerate	MaxClimb	D_1+F_U		1214.3	175.9	60
A350-941	ICAO_A	3	5	Accelerate	MaxClimb	D_1_U		1276.7	193	60
A350-941	ICAO_A	3	6	Accelerate	MaxClimb	D_ZERO		1418.4	215.4	60
A350-941	ICAO_A	3	7	Accelerate	MaxClimb	D_ZERO		1565	250	60
A350-941	ICAO_A	3	8	Climb	MaxClimb	D_ZERO	10000			
A350-941	ICAO_A	4	1	Takeoff	MaxTakeoff	D_1+F_D				
A350-941	ICAO_A	4	2	Climb	MaxTakeoff	D_1+F_U	1500			
A350-941	ICAO_A	4	3	Climb	MaxClimb	D_1+F_U	3000			
A350-941	ICAO_A	4	4	Accelerate	MaxClimb	D_1+F_U		1138.4	180.3	60
A350-941	ICAO_A	4	5	Accelerate	MaxClimb	D_1_U		1212.8	196.1	60
A350-941	ICAO_A	4	6	Accelerate	MaxClimb	D_ZERO		1340.5	217	60
A350-941	ICAO_A	4	7	Accelerate	MaxClimb	D_ZERO		1476.4	250	60
A350-941	ICAO_A	4	8	Climb	MaxClimb	D_ZERO	10000			
A350-941	ICAO_A	5	1	Takeoff	MaxTakeoff	D_1+F_D				
A350-941	ICAO_A	5	2	Climb	MaxTakeoff	D_1+F_U	1500			
A350-941	ICAO_A	5	3	Climb	MaxClimb	D_1+F_U	3000			
A350-941	ICAO_A	5	4	Accelerate	MaxClimb	D_1+F_U		1066.3	185.8	60
A350-941	ICAO_A	5	5	Accelerate	MaxClimb	D_1_U		1139.9	200.3	60
A350-941	ICAO_A	5	6	Accelerate	MaxClimb	D_ZERO		1252.3	219.5	60
A350-941	ICAO_A	5	7	Accelerate	MaxClimb	D_ZERO		1374.5	250	60
A350-941	ICAO_A	5	8	Climb	MaxClimb	D_ZERO	10000			
A350-941	ICAO_A	6	1	Takeoff	MaxTakeoff	D_1+F_D				
A350-941	ICAO_A	6	2	Climb	MaxTakeoff	D_1+F_U	1500			

A350-941	ICAO_A	6	3	Climb	MaxClimb	D_1+F_U	3000			
A350-941	ICAO_A	6	4	Accelerate	MaxClimb	D_1+F_U		994.4	191.7	60
A350-941	ICAO_A	6	5	Accelerate	MaxClimb	D_1_U		1064.9	204.8	60
A350-941	ICAO_A	6	6	Accelerate	MaxClimb	D_ZERO		1165.9	222.3	60
A350-941	ICAO_A	6	7	Accelerate	MaxClimb	D_ZERO		1275.1	250	60
A350-941	ICAO_A	6	8	Climb	MaxClimb	D_ZERO	10000			
A350-941	ICAO_A	7	1	Takeoff	MaxTakeoff	D_1+F_D				
A350-941	ICAO_A	7	2	Climb	MaxTakeoff	D_1+F_U	1500			
A350-941	ICAO_A	7	3	Climb	MaxClimb	D_1+F_U	3000			
A350-941	ICAO_A	7	4	Accelerate	MaxClimb	D_1+F_U		927	197.8	60
A350-941	ICAO_A	7	5	Accelerate	MaxClimb	D_1_U		994.4	209.7	60
A350-941	ICAO_A	7	6	Accelerate	MaxClimb	D_ZERO		1085.3	225.7	60
A350-941	ICAO_A	7	7	Accelerate	MaxClimb	D_ZERO		1181	250	60
A350-941	ICAO_A	7	8	Climb	MaxClimb	D_ZERO	10000			
A350-941	ICAO_A	8	1	Takeoff	MaxTakeoff	D_1+F_D				
A350-941	ICAO_A	8	2	Climb	MaxTakeoff	D_1+F_U	1500			
A350-941	ICAO_A	8	3	Climb	MaxClimb	D_1+F_U	3000			
A350-941	ICAO_A	8	4	Accelerate	MaxClimb	D_1+F_U		862.4	204.1	60
A350-941	ICAO_A	8	5	Accelerate	MaxClimb	D_1_U		927.4	214.9	60
A350-941	ICAO_A	8	6	Accelerate	MaxClimb	D_ZERO		1009.2	229.4	60
A350-941	ICAO_A	8	7	Accelerate	MaxClimb	D_ZERO		1091.2	250	60
A350-941	ICAO_A	8	8	Climb	MaxClimb	D_ZERO	10000			
A350-941	ICAO_A	M	1	Takeoff	MaxTakeoff	D_1+F_D				
A350-941	ICAO_A	M	2	Climb	MaxTakeoff	D_1+F_U	1500			
A350-941	ICAO_A	M	3	Climb	MaxClimb	D_1+F_U	3000			
A350-941	ICAO_A	M	4	Accelerate	MaxClimb	D_1+F_U		823.3	208.3	60
A350-941	ICAO_A	M	5	Accelerate	MaxClimb	D_1_U		886.5	218.4	60
A350-941	ICAO_A	M	6	Accelerate	MaxClimb	D_ZERO		963.5	232	60
A350-941	ICAO_A	M	7	Accelerate	MaxClimb	D_ZERO		1036.9	250	60
A350-941	ICAO_A	M	8	Climb	MaxClimb	D_ZERO	10000			
A350-941	ICAO_B	1	1	Takeoff	MaxTakeoff	D_1+F_D				
A350-941	ICAO_B	1	2	Climb	MaxTakeoff	D_1+F_D	1000			

A350-941	ICAO_B	1	3	Accelerate	MaxTakeoff	D_1+F_U		1726.5	170.7	60
A350-941	ICAO_B	1	4	Accelerate	MaxTakeoff	D_1_U		1862.6	197.2	60
A350-941	ICAO_B	1	5	Climb	MaxClimb	D_ZERO	3000			
A350-941	ICAO_B	1	6	Accelerate	MaxClimb	D_ZERO		1658	250	60
A350-941	ICAO_B	1	7	Climb	MaxClimb	D_ZERO	10000			
A350-941	ICAO_B	2	1	Takeoff	MaxTakeoff	D_1+F_D				
A350-941	ICAO_B	2	2	Climb	MaxTakeoff	D_1+F_D	1000			
A350-941	ICAO_B	2	3	Accelerate	MaxTakeoff	D_1+F_U		1699.9	173.1	60
A350-941	ICAO_B	2	4	Accelerate	MaxTakeoff	D_1_U		1812.6	198.6	60
A350-941	ICAO_B	2	5	Climb	MaxClimb	D_ZERO	3000			
A350-941	ICAO_B	2	6	Accelerate	MaxClimb	D_ZERO		1604.5	250	60
A350-941	ICAO_B	2	7	Climb	MaxClimb	D_ZERO	10000			
A350-941	ICAO_B	3	1	Takeoff	MaxTakeoff	D_1+F_D				
A350-941	ICAO_B	3	2	Climb	MaxTakeoff	D_1+F_D	1000			
A350-941	ICAO_B	3	3	Accelerate	MaxTakeoff	D_1+F_U		1662.2	175.6	60
A350-941	ICAO_B	3	4	Accelerate	MaxTakeoff	D_1_U		1762.3	200.1	60
A350-941	ICAO_B	3	5	Climb	MaxClimb	D_ZERO	3000			
A350-941	ICAO_B	3	6	Accelerate	MaxClimb	D_ZERO		1551.6	250	60
A350-941	ICAO_B	3	7	Climb	MaxClimb	D_ZERO	10000			
A350-941	ICAO_B	4	1	Takeoff	MaxTakeoff	D_1+F_D				
A350-941	ICAO_B	4	2	Climb	MaxTakeoff	D_1+F_U	1000			
A350-941	ICAO_B	4	3	Accelerate	MaxTakeoff	D_1+F_U		1586.1	179.9	60
A350-941	ICAO_B	4	4	Accelerate	MaxTakeoff	D_1_U		1679.8	202.7	60
A350-941	ICAO_B	4	5	Climb	MaxClimb	D_ZERO	3000			
A350-941	ICAO_B	4	6	Accelerate	MaxClimb	D_ZERO		1465.3	250	60
A350-941	ICAO_B	4	7	Climb	MaxClimb	D_ZERO	10000			
A350-941	ICAO_B	5	1	Takeoff	MaxTakeoff	D_1+F_D				
A350-941	ICAO_B	5	2	Climb	MaxTakeoff	D_1+F_U	1000			
A350-941	ICAO_B	5	3	Accelerate	MaxTakeoff	D_1+F_U		1491.7	185.3	60
A350-941	ICAO_B	5	4	Accelerate	MaxTakeoff	D_1_U		1586.9	206.4	60
A350-941	ICAO_B	5	5	Climb	MaxClimb	D_ZERO	3000			
A350-941	ICAO_B	5	6	Accelerate	MaxClimb	D_ZERO		1365.5	250	60

A350-941	ICAO_B	5	7	Climb	MaxClimb	D_ZERO	10000			
A350-941	ICAO_B	6	1	Takeoff	MaxTakeoff	D_1+F_D				
A350-941	ICAO_B	6	2	Climb	MaxTakeoff	D_1+F_U	1000			
A350-941	ICAO_B	6	3	Accelerate	MaxTakeoff	D_1+F_U		1399.5	191.1	60
A350-941	ICAO_B	6	4	Accelerate	MaxTakeoff	D_1_U		1494.1	210.4	60
A350-941	ICAO_B	6	5	Climb	MaxClimb	D_ZERO	3000			
A350-941	ICAO_B	6	6	Accelerate	MaxClimb	D_ZERO		1268.2	250	60
A350-941	ICAO_B	6	7	Climb	MaxClimb	D_ZERO	10000			
A350-941	ICAO_B	7	1	Takeoff	MaxTakeoff	D_1+F_D				
A350-941	ICAO_B	7	2	Climb	MaxTakeoff	D_1+F_U	1000			
A350-941	ICAO_B	7	3	Accelerate	MaxTakeoff	D_1+F_U		1314	197	60
A350-941	ICAO_B	7	4	Accelerate	MaxTakeoff	D_1_U		1407.1	214.7	60
A350-941	ICAO_B	7	5	Climb	MaxClimb	D_ZERO	3000			
A350-941	ICAO_B	7	6	Accelerate	MaxClimb	D_ZERO		1176.3	250	60
A350-941	ICAO_B	7	7	Climb	MaxClimb	D_ZERO	10000			
A350-941	ICAO_B	8	1	Takeoff	MaxTakeoff	D_1+F_D				
A350-941	ICAO_B	8	2	Climb	MaxTakeoff	D_1+F_U	1000			
A350-941	ICAO_B	8	3	Accelerate	MaxTakeoff	D_1+F_U		1233.3	203.4	60
A350-941	ICAO_B	8	4	Accelerate	MaxTakeoff	D_1_U		1325.3	219.6	60
A350-941	ICAO_B	8	5	Climb	MaxClimb	D_ZERO	3000			
A350-941	ICAO_B	8	6	Accelerate	MaxClimb	D_ZERO		1089.2	250	60
A350-941	ICAO_B	8	7	Climb	MaxClimb	D_ZERO	10000			
A350-941	ICAO_B	M	1	Takeoff	MaxTakeoff	D_1+F_D				
A350-941	ICAO_B	M	2	Climb	MaxTakeoff	D_1+F_U	1000			
A350-941	ICAO_B	M	3	Accelerate	MaxTakeoff	D_1+F_U		1185.1	207.6	60
A350-941	ICAO_B	M	4	Accelerate	MaxTakeoff	D_1_U		1275.6	222.9	60
A350-941	ICAO_B	M	5	Climb	MaxClimb	D_ZERO	3000			
A350-941	ICAO_B	M	6	Accelerate	MaxClimb	D_ZERO		1036.7	250	60
A350-941	ICAO_B	M	7	Climb	MaxClimb	D_ZERO	10000			

,

(h)   in Table I-4 (part 3), the following rows are added:

A350-941	DEFAULT	1	1	Takeoff	MaxTakeoff	D_1+F_D				
A350-941	DEFAULT	1	2	Climb	MaxTakeoff	D_1+F_D	1000			
A350-941	DEFAULT	1	3	Accelerate	MaxTakeoff	D_1+F_U		1726.5	170.7	60
A350-941	DEFAULT	1	4	Accelerate	MaxTakeoff	D_1_U		1862.6	197.2	60
A350-941	DEFAULT	1	5	Climb	MaxClimb	D_ZERO	3000			
A350-941	DEFAULT	1	6	Accelerate	MaxClimb	D_ZERO		1658	250	60
A350-941	DEFAULT	1	7	Climb	MaxClimb	D_ZERO	10000			
A350-941	DEFAULT	2	1	Takeoff	MaxTakeoff	D_1+F_D				
A350-941	DEFAULT	2	2	Climb	MaxTakeoff	D_1+F_D	1000			
A350-941	DEFAULT	2	3	Accelerate	MaxTakeoff	D_1+F_U		1699.9	173.1	60
A350-941	DEFAULT	2	4	Accelerate	MaxTakeoff	D_1_U		1812.6	198.6	60
A350-941	DEFAULT	2	5	Climb	MaxClimb	D_ZERO	3000			
A350-941	DEFAULT	2	6	Accelerate	MaxClimb	D_ZERO		1604.5	250	60
A350-941	DEFAULT	2	7	Climb	MaxClimb	D_ZERO	10000			
A350-941	DEFAULT	3	1	Takeoff	MaxTakeoff	D_1+F_D				
A350-941	DEFAULT	3	2	Climb	MaxTakeoff	D_1+F_D	1000			
A350-941	DEFAULT	3	3	Accelerate	MaxTakeoff	D_1+F_U		1662.2	175.6	60
A350-941	DEFAULT	3	4	Accelerate	MaxTakeoff	D_1_U		1762.3	200.1	60
A350-941	DEFAULT	3	5	Climb	MaxClimb	D_ZERO	3000			
A350-941	DEFAULT	3	6	Accelerate	MaxClimb	D_ZERO		1551.6	250	60
A350-941	DEFAULT	3	7	Climb	MaxClimb	D_ZERO	10000			
A350-941	DEFAULT	4	1	Takeoff	MaxTakeoff	D_1+F_D				
A350-941	DEFAULT	4	2	Climb	MaxTakeoff	D_1+F_U	1000			
A350-941	DEFAULT	4	3	Accelerate	MaxTakeoff	D_1+F_U		1586.1	179.9	60
A350-941	DEFAULT	4	4	Accelerate	MaxTakeoff	D_1_U		1679.8	202.7	60
A350-941	DEFAULT	4	5	Climb	MaxClimb	D_ZERO	3000			
A350-941	DEFAULT	4	6	Accelerate	MaxClimb	D_ZERO		1465.3	250	60
A350-941	DEFAULT	4	7	Climb	MaxClimb	D_ZERO	10000			
A350-941	DEFAULT	5	1	Takeoff	MaxTakeoff	D_1+F_D				
A350-941	DEFAULT	5	2	Climb	MaxTakeoff	D_1+F_U	1000			

A350-941	DEFAULT	5	3	Accelerate	MaxTakeoff	D_1+F_U		1491.7	185.3	60
A350-941	DEFAULT	5	4	Accelerate	MaxTakeoff	D_1_U		1586.9	206.4	60
A350-941	DEFAULT	5	5	Climb	MaxClimb	D_ZERO	3000			
A350-941	DEFAULT	5	6	Accelerate	MaxClimb	D_ZERO		1365.5	250	60
A350-941	DEFAULT	5	7	Climb	MaxClimb	D_ZERO	10000			
A350-941	DEFAULT	6	1	Takeoff	MaxTakeoff	D_1+F_D				
A350-941	DEFAULT	6	2	Climb	MaxTakeoff	D_1+F_U	1000			
A350-941	DEFAULT	6	3	Accelerate	MaxTakeoff	D_1+F_U		1399.5	191.1	60
A350-941	DEFAULT	6	4	Accelerate	MaxTakeoff	D_1_U		1494.1	210.4	60
A350-941	DEFAULT	6	5	Climb	MaxClimb	D_ZERO	3000			
A350-941	DEFAULT	6	6	Accelerate	MaxClimb	D_ZERO		1268.2	250	60
A350-941	DEFAULT	6	7	Climb	MaxClimb	D_ZERO	10000			
A350-941	DEFAULT	7	1	Takeoff	MaxTakeoff	D_1+F_D				
A350-941	DEFAULT	7	2	Climb	MaxTakeoff	D_1+F_U	1000			
A350-941	DEFAULT	7	3	Accelerate	MaxTakeoff	D_1+F_U		1314	197	60
A350-941	DEFAULT	7	4	Accelerate	MaxTakeoff	D_1_U		1407.1	214.7	60
A350-941	DEFAULT	7	5	Climb	MaxClimb	D_ZERO	3000			
A350-941	DEFAULT	7	6	Accelerate	MaxClimb	D_ZERO		1176.3	250	60
A350-941	DEFAULT	7	7	Climb	MaxClimb	D_ZERO	10000			
A350-941	DEFAULT	8	1	Takeoff	MaxTakeoff	D_1+F_D				
A350-941	DEFAULT	8	2	Climb	MaxTakeoff	D_1+F_U	1000			
A350-941	DEFAULT	8	3	Accelerate	MaxTakeoff	D_1+F_U		1233.3	203.4	60
A350-941	DEFAULT	8	4	Accelerate	MaxTakeoff	D_1_U		1325.3	219.6	60
A350-941	DEFAULT	8	5	Climb	MaxClimb	D_ZERO	3000			
A350-941	DEFAULT	8	6	Accelerate	MaxClimb	D_ZERO		1089.2	250	60
A350-941	DEFAULT	8	7	Climb	MaxClimb	D_ZERO	10000			
A350-941	DEFAULT	M	1	Takeoff	MaxTakeoff	D_1+F_D				
A350-941	DEFAULT	M	2	Climb	MaxTakeoff	D_1+F_U	1000			
A350-941	DEFAULT	M	3	Accelerate	MaxTakeoff	D_1+F_U		1185.1	207.6	60
A350-941	DEFAULT	M	4	Accelerate	MaxTakeoff	D_1_U		1275.6	222.9	60
A350-941	DEFAULT	M	5	Climb	MaxClimb	D_ZERO	3000			
A350-941	DEFAULT	M	6	Accelerate	MaxClimb	D_ZERO		1036.7	250	60

A350-941	DEFAULT	M	7	Climb	MaxClimb	D_ZERO	10000			
A350-941	ICAO_A	1	1	Takeoff	MaxTakeoff	D_1+F_D				
A350-941	ICAO_A	1	2	Climb	MaxTakeoff	D_1+F_U	1500			
A350-941	ICAO_A	1	3	Climb	MaxClimb	D_1+F_U	3000			
A350-941	ICAO_A	1	4	Accelerate	MaxClimb	D_1+F_U		1323.2	171	60
A350-941	ICAO_A	1	5	Accelerate	MaxClimb	D_1_U		1353.1	189.5	60
A350-941	ICAO_A	1	6	Accelerate	MaxClimb	D_ZERO		1514.1	213.7	60
A350-941	ICAO_A	1	7	Accelerate	MaxClimb	D_ZERO		1673.8	250	60
A350-941	ICAO_A	1	8	Climb	MaxClimb	D_ZERO	10000			
A350-941	ICAO_A	2	1	Takeoff	MaxTakeoff	D_1+F_D				
A350-941	ICAO_A	2	2	Climb	MaxTakeoff	D_1+F_U	1500			
A350-941	ICAO_A	2	3	Climb	MaxClimb	D_1+F_U	3000			
A350-941	ICAO_A	2	4	Accelerate	MaxClimb	D_1+F_U		1265.7	173.4	60
A350-941	ICAO_A	2	5	Accelerate	MaxClimb	D_1_U		1315.1	191.2	60
A350-941	ICAO_A	2	6	Accelerate	MaxClimb	D_ZERO		1466.2	214.5	60
A350-941	ICAO_A	2	7	Accelerate	MaxClimb	D_ZERO		1619.3	250	60
A350-941	ICAO_A	2	8	Climb	MaxClimb	D_ZERO	10000			
A350-941	ICAO_A	3	1	Takeoff	MaxTakeoff	D_1+F_D				
A350-941	ICAO_A	3	2	Climb	MaxTakeoff	D_1+F_U	1500			
A350-941	ICAO_A	3	3	Climb	MaxClimb	D_1+F_U	3000			
A350-941	ICAO_A	3	4	Accelerate	MaxClimb	D_1+F_U		1214.3	175.9	60
A350-941	ICAO_A	3	5	Accelerate	MaxClimb	D_1_U		1276.7	193	60
A350-941	ICAO_A	3	6	Accelerate	MaxClimb	D_ZERO		1418.4	215.4	60
A350-941	ICAO_A	3	7	Accelerate	MaxClimb	D_ZERO		1565	250	60
A350-941	ICAO_A	3	8	Climb	MaxClimb	D_ZERO	10000			
A350-941	ICAO_A	4	1	Takeoff	MaxTakeoff	D_1+F_D				
A350-941	ICAO_A	4	2	Climb	MaxTakeoff	D_1+F_U	1500			
A350-941	ICAO_A	4	3	Climb	MaxClimb	D_1+F_U	3000			
A350-941	ICAO_A	4	4	Accelerate	MaxClimb	D_1+F_U		1138.4	180.3	60
A350-941	ICAO_A	4	5	Accelerate	MaxClimb	D_1_U		1212.8	196.1	60
A350-941	ICAO_A	4	6	Accelerate	MaxClimb	D_ZERO		1340.5	217	60
A350-941	ICAO_A	4	7	Accelerate	MaxClimb	D_ZERO		1476.4	250	60

A350-941	ICAO_A	4	8	Climb	MaxClimb	D_ZERO	10000			
A350-941	ICAO_A	5	1	Takeoff	MaxTakeoff	D_1+F_D				
A350-941	ICAO_A	5	2	Climb	MaxTakeoff	D_1+F_U	1500			
A350-941	ICAO_A	5	3	Climb	MaxClimb	D_1+F_U	3000			
A350-941	ICAO_A	5	4	Accelerate	MaxClimb	D_1+F_U		1066.3	185.8	60
A350-941	ICAO_A	5	5	Accelerate	MaxClimb	D_1_U		1139.9	200.3	60
A350-941	ICAO_A	5	6	Accelerate	MaxClimb	D_ZERO		1252.3	219.5	60
A350-941	ICAO_A	5	7	Accelerate	MaxClimb	D_ZERO		1374.5	250	60
A350-941	ICAO_A	5	8	Climb	MaxClimb	D_ZERO	10000			
A350-941	ICAO_A	6	1	Takeoff	MaxTakeoff	D_1+F_D				
A350-941	ICAO_A	6	2	Climb	MaxTakeoff	D_1+F_U	1500			
A350-941	ICAO_A	6	3	Climb	MaxClimb	D_1+F_U	3000			
A350-941	ICAO_A	6	4	Accelerate	MaxClimb	D_1+F_U		994.4	191.7	60
A350-941	ICAO_A	6	5	Accelerate	MaxClimb	D_1_U		1064.9	204.8	60
A350-941	ICAO_A	6	6	Accelerate	MaxClimb	D_ZERO		1165.9	222.3	60
A350-941	ICAO_A	6	7	Accelerate	MaxClimb	D_ZERO		1275.1	250	60
A350-941	ICAO_A	6	8	Climb	MaxClimb	D_ZERO	10000			
A350-941	ICAO_A	7	1	Takeoff	MaxTakeoff	D_1+F_D				
A350-941	ICAO_A	7	2	Climb	MaxTakeoff	D_1+F_U	1500			
A350-941	ICAO_A	7	3	Climb	MaxClimb	D_1+F_U	3000			
A350-941	ICAO_A	7	4	Accelerate	MaxClimb	D_1+F_U		927	197.8	60
A350-941	ICAO_A	7	5	Accelerate	MaxClimb	D_1_U		994.4	209.7	60
A350-941	ICAO_A	7	6	Accelerate	MaxClimb	D_ZERO		1085.3	225.7	60
A350-941	ICAO_A	7	7	Accelerate	MaxClimb	D_ZERO		1181	250	60
A350-941	ICAO_A	7	8	Climb	MaxClimb	D_ZERO	10000			
A350-941	ICAO_A	8	1	Takeoff	MaxTakeoff	D_1+F_D				
A350-941	ICAO_A	8	2	Climb	MaxTakeoff	D_1+F_U	1500			
A350-941	ICAO_A	8	3	Climb	MaxClimb	D_1+F_U	3000			
A350-941	ICAO_A	8	4	Accelerate	MaxClimb	D_1+F_U		862.4	204.1	60
A350-941	ICAO_A	8	5	Accelerate	MaxClimb	D_1_U		927.4	214.9	60
A350-941	ICAO_A	8	6	Accelerate	MaxClimb	D_ZERO		1009.2	229.4	60
A350-941	ICAO_A	8	7	Accelerate	MaxClimb	D_ZERO		1091.2	250	60

A350-941	ICAO_A	8	8	Climb	MaxClimb	D_ZERO	10000			
A350-941	ICAO_A	M	1	Takeoff	MaxTakeoff	D_1+F_D				
A350-941	ICAO_A	M	2	Climb	MaxTakeoff	D_1+F_U	1500			
A350-941	ICAO_A	M	3	Climb	MaxClimb	D_1+F_U	3000			
A350-941	ICAO_A	M	4	Accelerate	MaxClimb	D_1+F_U		823.3	208.3	60
A350-941	ICAO_A	M	5	Accelerate	MaxClimb	D_1_U		886.5	218.4	60
A350-941	ICAO_A	M	6	Accelerate	MaxClimb	D_ZERO		963.5	232	60
A350-941	ICAO_A	M	7	Accelerate	MaxClimb	D_ZERO		1036.9	250	60
A350-941	ICAO_A	M	8	Climb	MaxClimb	D_ZERO	10000			
A350-941	ICAO_B	1	1	Takeoff	MaxTakeoff	D_1+F_D				
A350-941	ICAO_B	1	2	Climb	MaxTakeoff	D_1+F_D	1000			
A350-941	ICAO_B	1	3	Accelerate	MaxTakeoff	D_1+F_U		1726.5	170.7	60
A350-941	ICAO_B	1	4	Accelerate	MaxTakeoff	D_1_U		1862.6	197.2	60
A350-941	ICAO_B	1	5	Climb	MaxClimb	D_ZERO	3000			
A350-941	ICAO_B	1	6	Accelerate	MaxClimb	D_ZERO		1658	250	60
A350-941	ICAO_B	1	7	Climb	MaxClimb	D_ZERO	10000			
A350-941	ICAO_B	2	1	Takeoff	MaxTakeoff	D_1+F_D				
A350-941	ICAO_B	2	2	Climb	MaxTakeoff	D_1+F_D	1000			
A350-941	ICAO_B	2	3	Accelerate	MaxTakeoff	D_1+F_U		1699.9	173.1	60
A350-941	ICAO_B	2	4	Accelerate	MaxTakeoff	D_1_U		1812.6	198.6	60
A350-941	ICAO_B	2	5	Climb	MaxClimb	D_ZERO	3000			
A350-941	ICAO_B	2	6	Accelerate	MaxClimb	D_ZERO		1604.5	250	60
A350-941	ICAO_B	2	7	Climb	MaxClimb	D_ZERO	10000			
A350-941	ICAO_B	3	1	Takeoff	MaxTakeoff	D_1+F_D				
A350-941	ICAO_B	3	2	Climb	MaxTakeoff	D_1+F_D	1000			
A350-941	ICAO_B	3	3	Accelerate	MaxTakeoff	D_1+F_U		1662.2	175.6	60
A350-941	ICAO_B	3	4	Accelerate	MaxTakeoff	D_1_U		1762.3	200.1	60
A350-941	ICAO_B	3	5	Climb	MaxClimb	D_ZERO	3000			
A350-941	ICAO_B	3	6	Accelerate	MaxClimb	D_ZERO		1551.6	250	60
A350-941	ICAO_B	3	7	Climb	MaxClimb	D_ZERO	10000			
A350-941	ICAO_B	4	1	Takeoff	MaxTakeoff	D_1+F_D				
A350-941	ICAO_B	4	2	Climb	MaxTakeoff	D_1+F_U	1000			

A350-941	ICAO_B	4	3	Accelerate	MaxTakeoff	D_1+F_U		1586.1	179.9	60
A350-941	ICAO_B	4	4	Accelerate	MaxTakeoff	D_1_U		1679.8	202.7	60
A350-941	ICAO_B	4	5	Climb	MaxClimb	D_ZERO	3000			
A350-941	ICAO_B	4	6	Accelerate	MaxClimb	D_ZERO		1465.3	250	60
A350-941	ICAO_B	4	7	Climb	MaxClimb	D_ZERO	10000			
A350-941	ICAO_B	5	1	Takeoff	MaxTakeoff	D_1+F_D				
A350-941	ICAO_B	5	2	Climb	MaxTakeoff	D_1+F_U	1000			
A350-941	ICAO_B	5	3	Accelerate	MaxTakeoff	D_1+F_U		1491.7	185.3	60
A350-941	ICAO_B	5	4	Accelerate	MaxTakeoff	D_1_U		1586.9	206.4	60
A350-941	ICAO_B	5	5	Climb	MaxClimb	D_ZERO	3000			
A350-941	ICAO_B	5	6	Accelerate	MaxClimb	D_ZERO		1365.5	250	60
A350-941	ICAO_B	5	7	Climb	MaxClimb	D_ZERO	10000			
A350-941	ICAO_B	6	1	Takeoff	MaxTakeoff	D_1+F_D				
A350-941	ICAO_B	6	2	Climb	MaxTakeoff	D_1+F_U	1000			
A350-941	ICAO_B	6	3	Accelerate	MaxTakeoff	D_1+F_U		1399.5	191.1	60
A350-941	ICAO_B	6	4	Accelerate	MaxTakeoff	D_1_U		1494.1	210.4	60
A350-941	ICAO_B	6	5	Climb	MaxClimb	D_ZERO	3000			
A350-941	ICAO_B	6	6	Accelerate	MaxClimb	D_ZERO		1268.2	250	60
A350-941	ICAO_B	6	7	Climb	MaxClimb	D_ZERO	10000			
A350-941	ICAO_B	7	1	Takeoff	MaxTakeoff	D_1+F_D				
A350-941	ICAO_B	7	2	Climb	MaxTakeoff	D_1+F_U	1000			
A350-941	ICAO_B	7	3	Accelerate	MaxTakeoff	D_1+F_U		1314	197	60
A350-941	ICAO_B	7	4	Accelerate	MaxTakeoff	D_1_U		1407.1	214.7	60
A350-941	ICAO_B	7	5	Climb	MaxClimb	D_ZERO	3000			
A350-941	ICAO_B	7	6	Accelerate	MaxClimb	D_ZERO		1176.3	250	60
A350-941	ICAO_B	7	7	Climb	MaxClimb	D_ZERO	10000			
A350-941	ICAO_B	8	1	Takeoff	MaxTakeoff	D_1+F_D				
A350-941	ICAO_B	8	2	Climb	MaxTakeoff	D_1+F_U	1000			
A350-941	ICAO_B	8	3	Accelerate	MaxTakeoff	D_1+F_U		1233.3	203.4	60
A350-941	ICAO_B	8	4	Accelerate	MaxTakeoff	D_1_U		1325.3	219.6	60
A350-941	ICAO_B	8	5	Climb	MaxClimb	D_ZERO	3000			
A350-941	ICAO_B	8	6	Accelerate	MaxClimb	D_ZERO		1089.2	250	60

A350-941	ICAO_B	8	7	Climb	MaxClimb	D_ZERO	10000			
A350-941	ICAO_B	M	1	Takeoff	MaxTakeoff	D_1+F_D				
A350-941	ICAO_B	M	2	Climb	MaxTakeoff	D_1+F_U	1000			
A350-941	ICAO_B	M	3	Accelerate	MaxTakeoff	D_1+F_U		1185.1	207.6	60
A350-941	ICAO_B	M	4	Accelerate	MaxTakeoff	D_1_U		1275.6	222.9	60
A350-941	ICAO_B	M	5	Climb	MaxClimb	D_ZERO	3000			
A350-941	ICAO_B	M	6	Accelerate	MaxClimb	D_ZERO		1036.7	250	60
A350-941	ICAO_B	M	7	Climb	MaxClimb	D_ZERO	10000			
ATR72	DEFAULT	1	1	Takeoff	MaxTakeoff	15				
ATR72	DEFAULT	1	2	Climb	MaxTakeoff	15	1000			
ATR72	DEFAULT	1	3	Accelerate	MaxClimb	INTR		885	133.3	39.1
ATR72	DEFAULT	1	4	Accelerate	MaxClimb	ZERO		1040	142.4	35.6
ATR72	DEFAULT	1	5	Climb	MaxClimb	ZERO	3000			
ATR72	DEFAULT	1	6	Accelerate	MaxClimb	ZERO		964	168.3	38.9
ATR72	DEFAULT	1	7	Climb	MaxClimb	ZERO	5500			
ATR72	DEFAULT	1	8	Climb	MaxClimb	ZERO	7500			
ATR72	DEFAULT	1	9	Climb	MaxClimb	ZERO	10000			
ATR72	DEFAULT	2	1	Takeoff	MaxTakeoff	15				
ATR72	DEFAULT	2	2	Climb	MaxTakeoff	15	1000			
ATR72	DEFAULT	2	3	Accelerate	MaxClimb	INTR		900	138	31.7
ATR72	DEFAULT	2	4	Accelerate	MaxClimb	ZERO		995	147.3	32.2
ATR72	DEFAULT	2	5	Climb	MaxClimb	ZERO	3000			
ATR72	DEFAULT	2	6	Accelerate	MaxClimb	ZERO		962	168.3	32.1
ATR72	DEFAULT	2	7	Climb	MaxClimb	ZERO	5500			
ATR72	DEFAULT	2	8	Climb	MaxClimb	ZERO	7500			
ATR72	DEFAULT	2	9	Climb	MaxClimb	ZERO	10000			
ATR72	DEFAULT	3	1	Takeoff	MaxTakeoff	15				
ATR72	DEFAULT	3	2	Climb	MaxTakeoff	15	1000			
ATR72	DEFAULT	3	3	Accelerate	MaxClimb	INTR		890	139.8	24.5
ATR72	DEFAULT	3	4	Accelerate	MaxClimb	ZERO		942	149.2	27.9
ATR72	DEFAULT	3	5	Climb	MaxClimb	ZERO	3000			
ATR72	DEFAULT	3	6	Accelerate	MaxClimb	ZERO		907	168.3	27.8

ATR72	DEFAULT	3	7	Climb	MaxClimb	ZERO	5500			
ATR72	DEFAULT	3	8	Climb	MaxClimb	ZERO	7500			
ATR72	DEFAULT	3	9	Climb	MaxClimb	ZERO	10000			

'

(i)   in Table I-6, the following rows are added:

'

7378MAX	1	140000
7378MAX	2	144600
7378MAX	3	149600
7378MAX	4	159300
7378MAX	5	171300
7378MAX	6	174500
7378MAX	M	181200
A350-941	1	421680
A350-941	2	433189
A350-941	3	445270
A350-941	4	466326
A350-941	5	493412
A350-941	6	522377
A350-941	7	552871
A350-941	8	585147
A350-941	M	606271
ATR72	1	44750
ATR72	2	47620
ATR72	3	50710

'

(j)   in Table I-7, after the row

"

737800	MaxTkoffHiTemp	30143.2	-29.773	-0.029	0	-145.2				

"

the following rows are added:

'

737800	IdleApproach	649.0	-3.3	0.0118	0	0				
7378MAX	IdleApproach	1046	-4.6	0.0147	0	0				
7378MAX	MaxClimb	21736	-28.6	0.3333	-3.28E-06	0				
7378MAX	MaxClimbHiTemp	23323	-15.1	-0.09821	6.40E-06	-142.0575				
7378MAX	MaxTakeoff	26375	-32.3	0.07827	8.81E-07	0				
7378MAX	MaxTkoffHiTemp	30839	-27.1	-0.06346	-8.23E-06	-183.1101				
A350-941	IdleApproach	5473.2	-24.305716	0.0631198	-4.21E-06	0				
A350-941	IdleApproachHiTemp	5473.2	-24.305716	0.0631198	-4.21E-06	0				
A350-941	MaxClimb	67210.9	-82.703367	1.18939	-0.000012074	0				
A350-941	MaxClimbHiTemp	76854. 6	-75.672429	0	0	-466				
A350-941	MaxTakeoff	84912.8	-101.986997	0.940876	-8.31E-06	0				
A350-941	MaxTkoffHiTemp	96170.0	-101.339623	0	0	-394				
ATR72	MaxClimb	5635.2	-9.5	0.01127	0.00000027	0				
ATR72	MaxTakeoff	7583.5	-20.3	0.137399	-0.00000604	0				

'

(k)   in Table I-9, the following rows are added:

'

7378MAX	LAmax	A	3000	90.4	83.4	78.7	73.8	65.9	57.1	50.7	43.6	36.5	29.7
7378MAX	LAmax	A	4000	90.5	83.4	78.8	73.8	65.9	57.1	50.6	43.5	36.4	29.6
7378MAX	LAmax	A	5000	90.7	83.7	79	74.1	66.1	57.2	50.7	43.6	36.5	29.6
7378MAX	LAmax	A	6000	91	84	79.4	74.4	66.5	57.6	51	43.9	36.7	29.9
7378MAX	LAmax	A	7000	91.5	84.4	79.8	74.8	66.9	58	51.5	44.3	37.1	30.2
7378MAX	LAmax	D	10000	92.4	85.8	81.4	76.6	68.9	60.2	53.9	46.8	39.7	33

7378MAX	LAmax	D	13000	94.2	87.7	83.2	78.4	70.7	62	55.6	48.5	41.4	34.6
7378MAX	LAmax	D	16000	96	89.4	84.9	80.1	72.4	63.7	57.3	50.3	43.2	36.5
7378MAX	LAmax	D	19000	97.6	91	86.5	81.8	74	65.3	59	52.1	45.1	38.4
7378MAX	LAmax	D	22000	99.2	92.6	88.1	83.4	75.6	67	60.8	54	47.1	40.5
7378MAX	LAmax	D	24500	100.6	94	89.5	84.8	77	68.5	62.4	55.7	48.9	42.5
7378MAX	SEL	A	3000	92.6	88.4	85.6	82.4	77.2	70.9	66.1	60.8	55.4	50.2
7378MAX	SEL	A	4000	92.7	88.6	85.8	82.6	77.3	71	66.2	60.9	55.5	50.4
7378MAX	SEL	A	5000	93	88.9	86.1	82.9	77.6	71.3	66.5	61.1	55.7	50.6
7378MAX	SEL	A	6000	93.3	89.3	86.4	83.2	77.9	71.6	66.8	61.4	56	50.8
7378MAX	SEL	A	7000	93.7	89.6	86.8	83.6	78.3	72	67.1	61.8	56.3	51.1
7378MAX	SEL	D	10000	94.3	90.4	87.6	84.5	79.1	72.9	68.3	63.2	58	53.1
7378MAX	SEL	D	13000	96.1	92.2	89.4	86.3	80.8	74.5	69.9	64.8	59.6	54.8
7378MAX	SEL	D	16000	97.6	93.7	90.9	87.8	82.5	76.3	71.7	66.7	61.6	56.9
7378MAX	SEL	D	19000	98.8	95	92.3	89.3	84	78	73.6	68.7	63.8	59.1
7378MAX	SEL	D	22000	100	96.2	93.6	90.6	85.6	79.8	75.5	70.8	66.1	61.7
7378MAX	SEL	D	24500	100.9	97.2	94.6	91.7	86.9	81.4	77.4	72.8	68.3	64.1
A350-941	LAmax	A	1000	91.21	84.42	79.83	74.97	67.15	58.68	52.65	46.06	38.92	31.73
A350-941	LAmax	A	10000	92.16	85.43	80.83	75.99	68.31	59.92	53.97	47.34	40.08	32.68
A350-941	LAmax	A	17000	94.76	87.92	83.18	78.16	70.23	61.75	55.72	49.06	41.55	33.91
A350-941	LAmax	D	25000	92.83	85.22	80.6	75.75	68.22	60	54.03	47.27	39.73	31.65
A350-941	LAmax	D	35000	95.16	88.13	83.33	78.27	70.38	61.9	55.87	49.15	41.66	33.82
A350-941	LAmax	D	50000	99.67	92.61	87.75	82.5	74.45	66.01	60	53.34	45.7	37.42
A350-941	LAmax	D	70000	103.74	96.78	91.98	86.87	78.8	70.01	63.7	56.71	48.8	40.63
A350-941	SEL	A	1000	94.18	89.98	86.96	83.74	78.42	72.25	67.64	62.45	56.7	50.92
A350-941	SEL	A	10000	95.52	91.32	88.29	85.06	79.78	73.75	69.24	64.17	58.36	52.34
A350-941	SEL	A	17000	97.74	93.39	90.3	87.01	81.68	75.62	71.18	66.09	60.23	54
A350-941	SEL	D	25000	95.67	90.95	87.67	84.23	78.73	72.73	68.33	63.24	57.19	50.52
A350-941	SEL	D	35000	97.28	92.81	89.7	86.39	81.04	75.18	70.92	65.83	59.85	53.36
A350-941	SEL	D	50000	100.98	96.76	93.79	90.43	85.11	79.2	74.81	69.77	63.84	57.37
A350-941	SEL	D	70000	104.66	100.74	97.82	94.68	89.49	83.56	79.09	73.94	67.84	61.27
ATR72	LAmax	A	890	86.6	79.4	74.4	69.2	61.1	52.5	46.6	40	32.7	25
ATR72	LAmax	A	900	86.6	79.4	74.4	69.2	61.1	52.5	46.6	40	32.7	25

ATR72	LAmax	A	1250	86.7	79.5	74.5	69.3	61.2	52.6	46.6	40	32.6	24.8
ATR72	LAmax	A	1600	87.5	80.2	75.1	69.9	61.9	53.4	47.4	40.8	33.4	25.7
ATR72	LAmax	D	3000	87.7	81.1	76.7	71.9	64.4	56.7	50.9	44.1	37.2	29.9
ATR72	LAmax	D	3600	89.4	82.8	78.6	73.9	66.3	58	52.2	45.5	38.8	31.5
ATR72	LAmax	D	4200	91.1	84.5	80.6	75.9	68.2	59.8	53.9	47.1	40.2	32.9
ATR72	LAmax	D	4800	92.8	86.3	82.5	77.9	70.1	62.1	56	48.8	41.5	33.8
ATR72	LAmax	D	4900	94.6	88.2	84	79.7	72.9	65.7	60.8	55.3	50	43.9
ATR72	LAmax	D	5300	95.7	89.5	85.2	81	74.3	67.3	62.4	57	51.7	45.6
ATR72	LAmax	D	5310	95.7	89.5	85.2	81	74.3	67.3	62.4	57	51.7	45.6
ATR72	SEL	A	890	89.7	85	81.7	78.2	72.8	66.9	62.6	57.7	52.1	45.9
ATR72	SEL	A	900	89.7	85	81.7	78.2	72.8	66.9	62.6	57.7	52.1	45.9
ATR72	SEL	A	1250	89.4	84.7	81.5	78.1	72.8	66.8	62.5	57.6	51.8	45.6
ATR72	SEL	A	1600	89.7	85.1	81.8	78.4	73.1	67.3	63	58.1	52.4	46.2
ATR72	SEL	D	3000	88.9	84.8	82	79	74.3	68.9	64.9	60	54.6	48.6
ATR72	SEL	D	3600	90	85.9	83.2	80.3	75.5	70.3	66.4	61.6	56.4	50.5
ATR72	SEL	D	4200	91.1	87.1	84.4	81.6	77	71.9	67.9	63	57.8	51.9
ATR72	SEL	D	4800	92.2	88.2	85.6	82.9	78.8	73.8	69.6	64.4	58.8	52.7
ATR72	SEL	D	4900	92.9	89.4	86.9	84.3	80.3	75.9	72.9	69.3	65.5	61.3
ATR72	SEL	D	5300	93.7	90.2	87.7	85.2	81.4	77.1	74.1	70.6	66.8	62.6
ATR72	SEL	D	5310	93.7	90.2	87.7	85.2	81.4	77.1	74.1	70.6	66.8	62.6

,

(l)   in Table I-10, the following rows are inserted after the row corresponding to "Spectral Class ID" number 138:

'

139	Departure	2-Engine.HighByPass.Tfan	71,4	67,4	59,1	69,3	75,3	76,7	72,6	69,3	76,4	71,2	71,8
140	Departure	2-Engine.Tprop	63,5	62,8	71,0	87,4	78,5	76,8	74,6	77,4	79,8	74,3	75,4

,

(m)   in Table I-10, the following rows are added:

'

| 239 | Approach | 2-Engine.HighByPass.Tfan | 71,0 | 65,0 | 60,7 | 70,7 | 74,8 | 76,5 | 73,2 | 71,8 | 75,9 | 73,0 | 71,1 |
| 240 | Approach | 2-Engine.Tprop | 65,9 | 68,0 | 66,9 | 80,0 | 77,1 | 78,5 | 73,9 | 75,6 | 77,7 | 73,6 | 73,3 |

'